RESEARCH ARTICLE

Development of efficient plasmid DNA transfer into adult rat central nervous system using microbubble-enhanced ultrasound

M Shimamura[1,2], N Sato[1], Y Taniyama[1], S Yamamoto[2], M Endoh[2], H Kurinami[3], M Aoki[3], T Ogihara[3], Y Kaneda[2] and R Morishita[1]

[1]Division of Clinical Gene Therapy, Osaka University, Yamada-oka, Suita, Japan; [2]Division of Gene Therapy Science, Osaka University, Yamada-oka, Suita, Japan; and [3]Department of Geriatric Medicine, Graduate School of Medicine, Osaka University, Yamada-oka, Suita, Japan

Although gene therapy might become a promising approach for central nervous system diseases, the safety issue is a serious consideration in human gene therapy. To overcome this problem, we developed an efficient gene transfer method into the adult rat brain based on plasmid DNA using a microbubble-enhanced ultrasound method, since microbubble-enhanced ultrasound has shown promise for transfecting genes into other tissues such as blood vessels. Using the microbubble-enhanced ultrasound method, luciferase expression was increased approximately 10-fold as compared to injection of naked plasmid DNA alone. Interestingly, the site of gene expression was limited to the site of insonation with intracisternal injection, in contrast to previous studies using viruses. Expression of the reporter gene, Venus, was readily detected in the central nervous system. The transfected cells were mainly detected in meningeal cells with intracisternal injection, and in glial cells with intrastriatal injection. There was no obvious evidence of tissue damage by microbubble-enhanced ultrasound. Overall, the present study demonstrated the feasibility of efficient plasmid DNA transfer into the central nervous system, providing a new option for treating various diseases such as tumors.
Gene Therapy (2004) 11, 1532–1539. doi:10.1038/sj.gt.3302323; Published online 22 July 2004

Keywords: *central nervous system; naked DNA; microbubble; ultrasound*

Introduction

Gene therapy for the central nervous system is a promising approach to treat central nervous system diseases. In fact, novel gene therapy has been tried clinically for glioblastoma,[1,2] Parkinson's disease,[3] and Canavan's disease.[4] In these trials, adenovirus and adeno-associated virus (AAV) were commonly used. However, there are serious safety problems in the case of viral vectors, such as immunogenicity,[5] delayed demyelination,[6] and difficulties in the preparation of a high titer of virus.[7] Since naked plasmid DNA is safe and easy to handle as compared to viral vectors, intramuscular injection of naked plasmid DNA of angiogenic growth factors such as vascular growth factor (VEGF) has been used clinically for the treatment of ischemic cardiovascular disease.[8,9] Although some researchers have tried to apply direct injection of naked plasmid DNA into the brain,[10,11] the transfection efficiency was quite low[10] and a large amount of naked plasmid DNA was required to produce the target protein.[11]

Recently, ultrasound-mediated gene transfer has been reported to augment the transfection efficiency and

Correspondence: Professor R Morishita, Division of Clinical Gene Therapy, Graduate School of Medicine, Osaka University, 2-2 Yamada-oka, Suita 565-0871, Japan

facilitate local gene expression.[12] Interestingly, gene transfer into the fetal central nervous system was successfully achieved by intrauterine injection with microbubble-enhanced ultrasound.[13] Compared to other viral vectors, there are some theoretical advantages including safety, simplicity of preparation, and local gene transfer. Thus, we focused on the development of gene transfer using naked plasmid DNA with an ultrasound or microbubble-enhanced ultrasound method. In the present study, we investigated the possibility of improving plasmid DNA-based gene transfer into the rat brain.
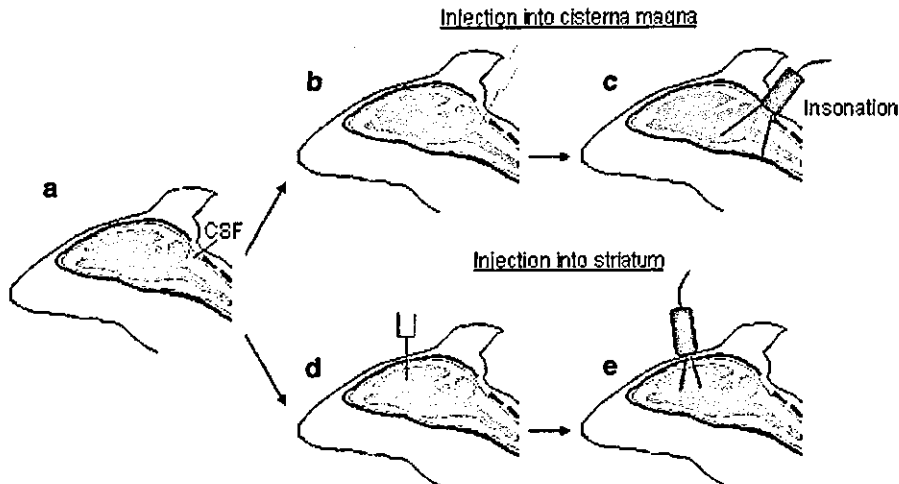
Results
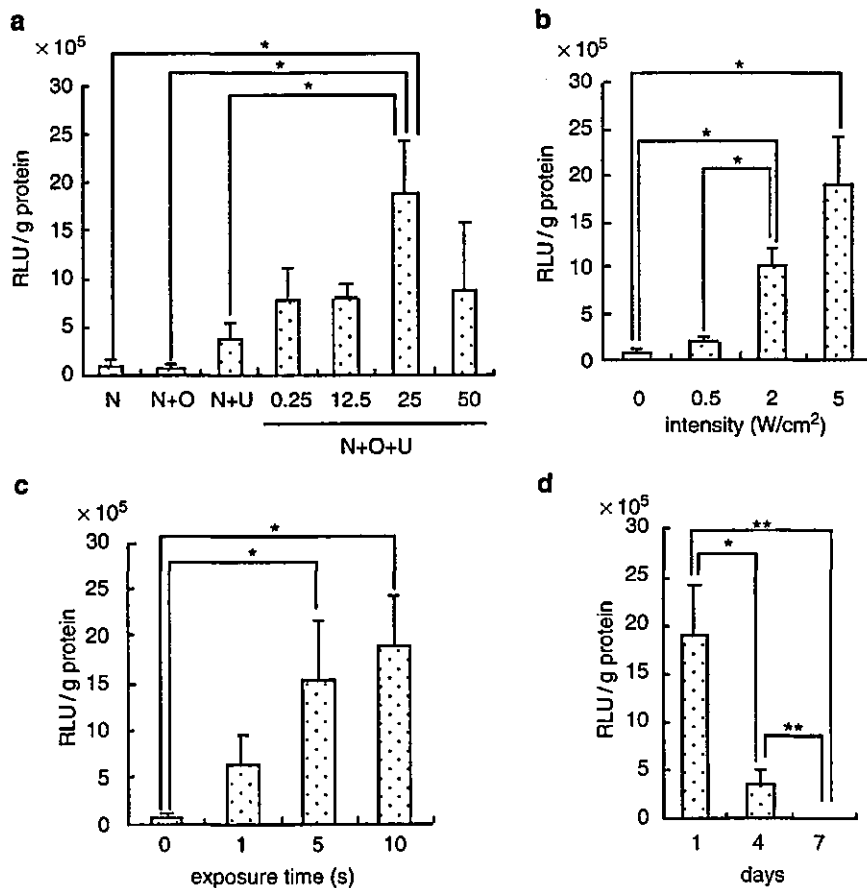
Gene transfer via cisterna magna

First, we measured luciferase activity in the brainstem and cerebellum after injection of the luciferase gene into the cisterna magna (Figure 1a–c). Although luciferase activity could be detected following injection of naked DNA alone, it was very low (Figure 2a). Insonation without microbubbles, Optison, after injection of naked DNA showed a tendency for an increase in luciferase activity. As expected, luciferase activity was markedly enhanced by the addition of 25% Optison and ultrasound (Figure 2a, $P < 0.05$), while addition of Optison alone without insonation did not affect luciferase activity.

Injection into cisterna magna

Injection into striatum

Figure 1 Schematic diagram of injection and insonation. For gene transfer via the cisterna magna, a mixture of naked plasmid DNA and Optison was injected (b) and animals were exposed to ultrasound (c). For gene transfer into the striatum or lateral ventricle, the solution was injected stereotactically (d), and animals were insonated via the hole (e).

Figure 2 Efficacy using ultrasound after injection of naked plasmid DNA into cisterna magna (subarachnoid space). Luciferase activity in the brainstem and cerebellum was measured 1 day (a–d) or 4 and 7 days (d) after injection of the luciferase gene into the subarachnoid space via the cisterna magna. (a) Optison was added to the vector at a concentration of 6.25, 12.5, 25, or 50% of total volume (100 µl). The ultrasound conditions were fixed as follows: intensity 5 W/cm²; exposure time 10 s. N: naked plasmid DNA alone; N+O: injected with a mixture of naked plasmid DNA and Optison (25%); N+U: insonated after injection of naked DNA alone; N+O+U: insonated after injection of a mixture of naked plasmid DNA and Optison. (b) Influence of intensity (Optison 25%, exposure time 10 s). (c) Influence of exposure time (Optison 25%, intensity 5 W/cm²). (d) Time course of gene expression (Optison 25%, intensity 5 W/cm², exposure time 10 s). *P <0.05, **P <0.01. n =4 for each group.

Although an increase in luciferase activity by addition of 6.25, 12.5, or 50% Optison was also observed, the most effective dose was 25% (Figure 2a). An increase in intensity of ultrasound also increased luciferase activity. An intensity of ultrasound of 5 W/cm² was adequate for high transfection efficiency (Figure 2b). In addition, an increase in the exposure time of ultrasound up to 10 s enhanced the transfection efficiency (Figure 2c). According to these results, the following experiments were performed under the optimal conditions of 25% Optison, 10 s duration, and 5 W/cm². Unexpectedly, the period of expression of the transgene was relatively short, and at 7 days after transfection, luciferase activity had almost returned to an undetectable level (Figure 2d).

To examine which cells could be transfected, we transfected the Venus gene into the cisterna magna. In contrast to previous data using vectors such as adenovirus, gene expression was limited to the brainstem and cerebellum, where insonation was performed (Figure 3d). There was no gene expression in the cerebral surface (Figure 3b), striatum, or choroid plexus in the lateral ventricle (Figure 3c). Coronal sections of the brainstem showed readily detectable fluorescence of Venus in meningeal cells in the pia mater and arachnoid membrane (Figure 3e and f). Consistent with the expression of the Venus gene, luciferase activity was also detected only in the brainstem and cerebellum (Figure 4).

Gene transfer into striatum

Next, the luciferase gene was directly injected into the striatum (Figure 1d and e). Although luciferase expression was detected following injection of the naked luciferase gene alone (Figure 5a), it was very low. The expression was enhanced about three-fold by addition of ultrasound, and about 10-fold by the addition of 25% Optison and ultrasound (Figure 5a, $P<0.01$). Since there could be strong absorption of ultrasound by the cranium, we further evaluated the optimal ultrasound conditions. Luciferase activity was maximal at 5 W/cm² (Figure 5b) and an exposure duration of 10 s (Figure 5c). According to these results, the following experiments were performed using the optimal ultrasound conditions of 5 W/cm² and 10 s duration. Gene expression was observed at least 14 days after injection, which was different from the result of intracisternal injection (Figure 5d). Then, we injected the Venus gene (50 µg) to clarify the transfectable cells. Transfected cells could not be detected at the injection site with naked plasmid DNA alone. In contrast, gene expression was successfully detected at the injection site using microbubble-enhanced ultrasound (Figure 6a). Immunohistochemical staining for NeuN revealed that the transfected cells were not neurons (Figure 6c).

Safety evaluation

The safety of Optison and ultrasound for gene transfer in the CNS is a critical issue. Since previous studies showed destruction of the blood–brain barrier (BBB) several hours after injection of Optison into the carotid artery[14] or insonation after intravenous injection of Optison,[15] we carefully evaluated the safety aspect of the present gene transfer method. We first evaluated the change in body weight, tissue damage by hematoxylin and eosin (HE) staining, and destruction of the BBB by microangiography using albumin–fluorescein isothiocyanate (FITC-albumin),[16] as the microbubble-enhanced ultrasound
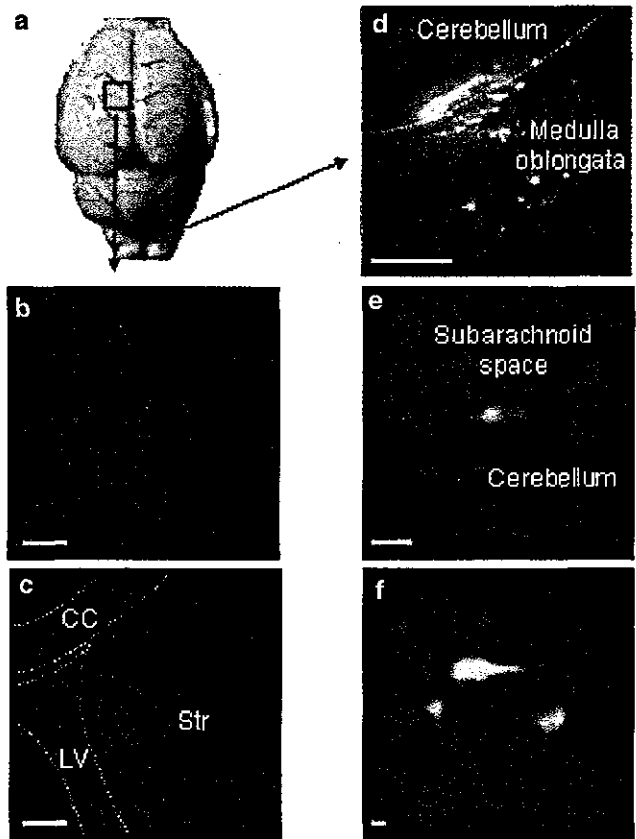

Figure 3 Typical example of transfected cells by plasmid DNA transfer using microbubble-enhanced ultrasound. Fluorescent stereomicroscopic image (b: surface of cerebral cortex; c: coronal section at the level of striatum; d: surface of cerebellum and medulla oblongata) and laser scanning confocal microscopic images (e, f) of Venus gene expression. Gene expression was observed only in the cerebellum and medulla oblongata, which were the injection sites (d). Coronal sections showed gene expression in meningeal cells in the pia mater (e) and arachnoid membrane (f). CC: corpus callosum; LV: lateral ventricle; Str: striatum. (b–d: bar = 0.5 mm; e, f: bar = 10 µm.)
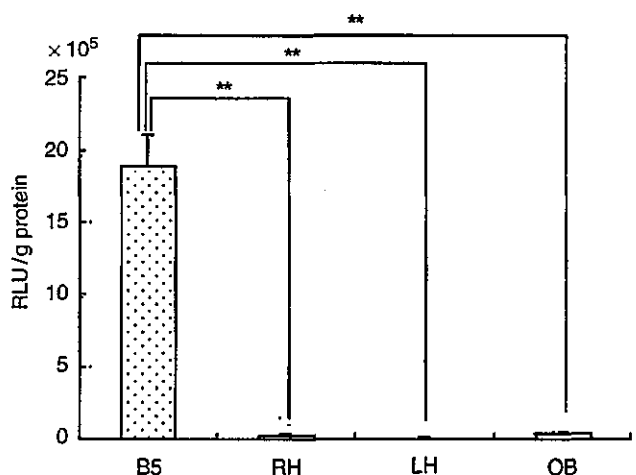

Figure 4 Local gene expression produced by plasmid DNA transfer using microbubble-enhanced ultrasound as assessed by luciferase expression. Luciferase activity was measured in the brainstem and cerebellum, left hemisphere, right hemisphere, and olfactory bulb at 1 day after transfection. Gene expression was limited to the brainstem and cerebellum, which were insonated. BS: brainstem and cerebellum; LH: left hemisphere; RH: right hemisphere; OB: olfactory bulb. **P <0.01. n = 4 for each group.
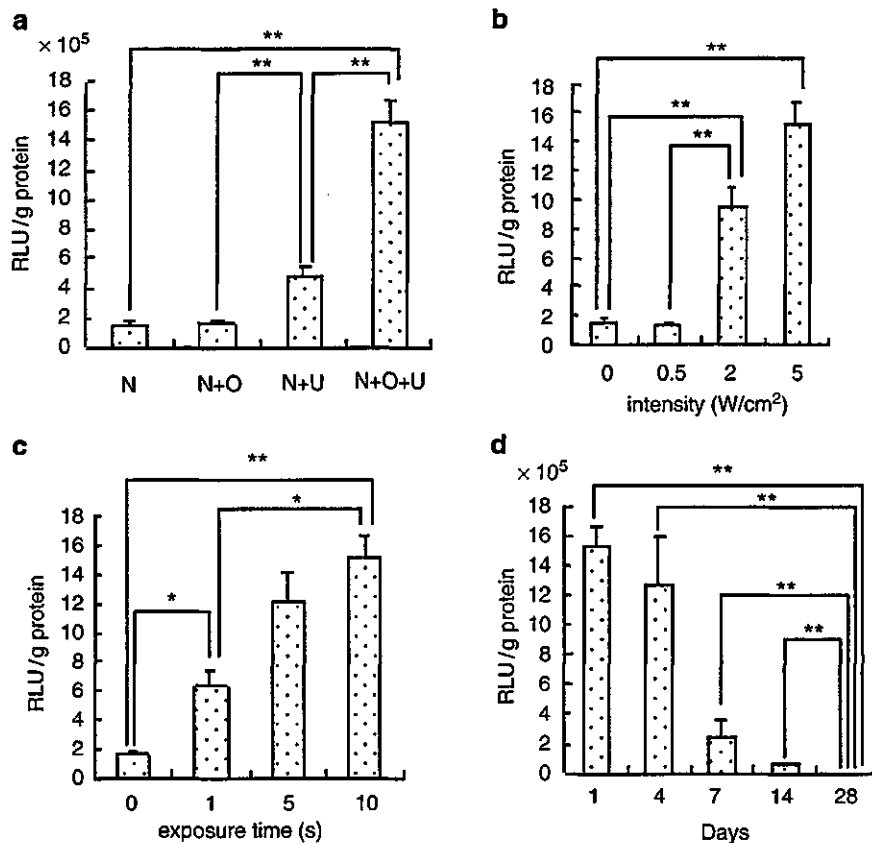
Figure 5 Effect of microbubble-enhanced ultrasound after injection of naked plasmid DNA into striatum. Luciferase activity was measured at 1 day after transfer of luciferase gene into the striatum. The Optison concentration was fixed at 25%. (a) Effect of ultrasound and/or Optison on luciferase activity. (b) Influence of intensity (Optison 25%, exposure time 10 s). (c) Influence of exposure time (Optison 25%, intensity 5 W/cm²). (d) Time course of luciferase gene expression. N: naked plasmid DNA alone; N+O: mixture of naked plasmid DNA and Optison (25%); N+U: insonation after injection of naked DNA alone; N+O+US: treatment with insonation after injection of a mixture of naked plasmid DNA and Optison. *P<0.05, **P<0.01. n=4 for each group.
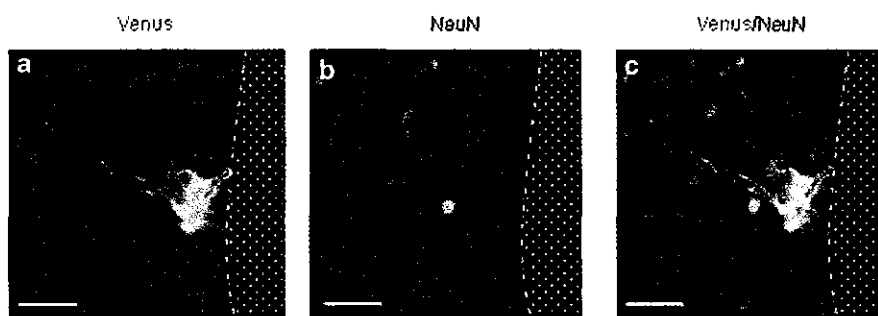
Figure 6 Typical example of transfected cells after injection of naked DNA into striatum with microbubble-enhanced ultrasound. Venus expression was observed by confocal imaging. Transfected cells are observed adjacent to the injection site (a). The transfected cells were not positive for NeuN (b, c). The dotted area indicates the needle track. (Bar = 50 μm.).

method achieved high transfection efficiency via a transient change in the cell membrane.[12,13]

Although body weight was decreased temporarily after each treatment, there was no significant difference among the groups (Figure 7). There was no histological change or leakage of FITC-albumin in the brainstem and cerebellum after intracisternal injection and insonation (Figures 8a–c and 9a–c). Although there was hemorrhage at the injection site with intrastriatal injection, the damage was not worsened by Optison or ultrasound (Figure 8d–f). The damage had not extended at least 28

days after injection (Figure 8f). There was slight leakage of FITC-albumin at the injection site (dim green area around vessels), but microbubble-enhanced ultrasound did not worsen the leakage (Figure 9d–f). No behavioral abnormality was observed.

Discussion

The most critical aspect of human gene therapy is the safety of vectors, although the efficiency of transfection
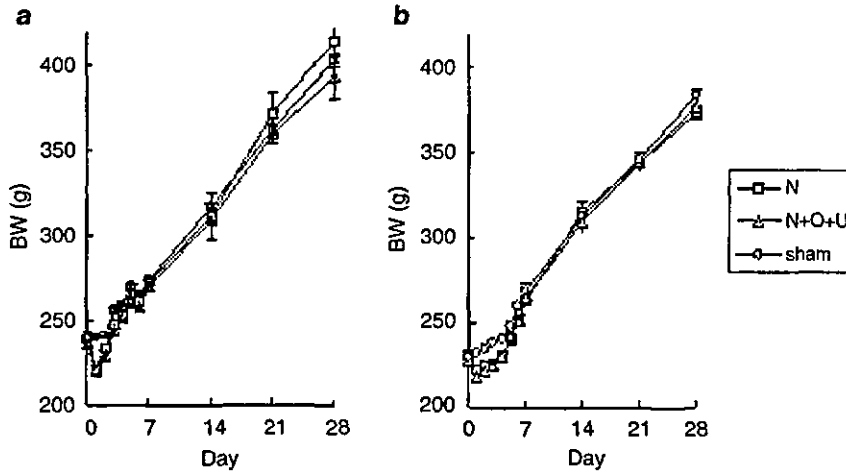
Figure 7 Effect of microbubble-enhanced ultrasound method on body weight. Body weight was measured after intracisternal injection of luciferase plasmid DNA via the cisterna magna (a) and intrastriatal injection (b). There was no significant difference among the groups. Sham: anesthetized rats without injection; N: rats transfected with naked plasmid DNA alone; N+O+U: rats insonated after injection of a mixture of naked plasmid DNA and Optison (25%). Ultrasound conditions: intensity 5 W/cm²; exposure time 10 s. n = 3 for each group.
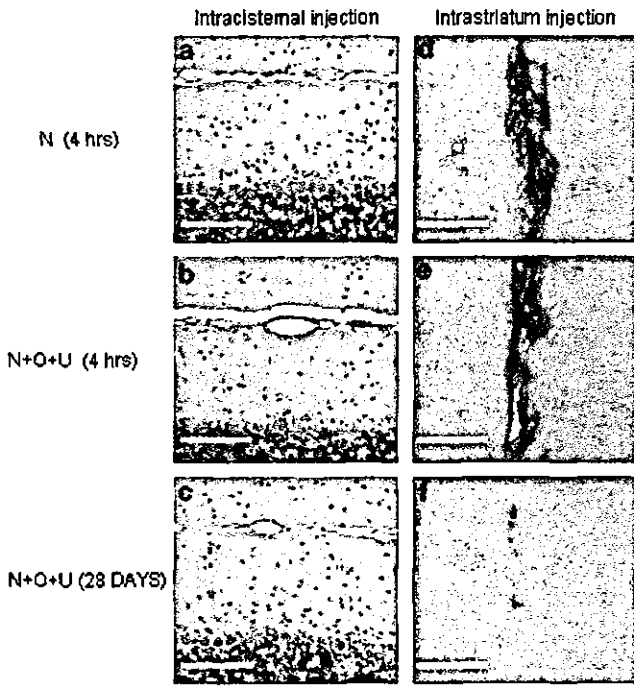
Figure 8 Hematoxylin and eosin (HE) staining after injection of naked DNA into cisterna magna or striatum with microbubble-enhanced ultrasound method. There was no histological change such as hemorrhage after intracisternal injection in both the acute phase (a, b) and chronic phase (c). Following intrastriatal injection, limited hemorrhage at the injection site was observed in the acute phase (d, e). However, there was no exacerbation by adding Optison and ultrasound. The damage had not extended in the chronic stage (f). Bar = 100 μm.
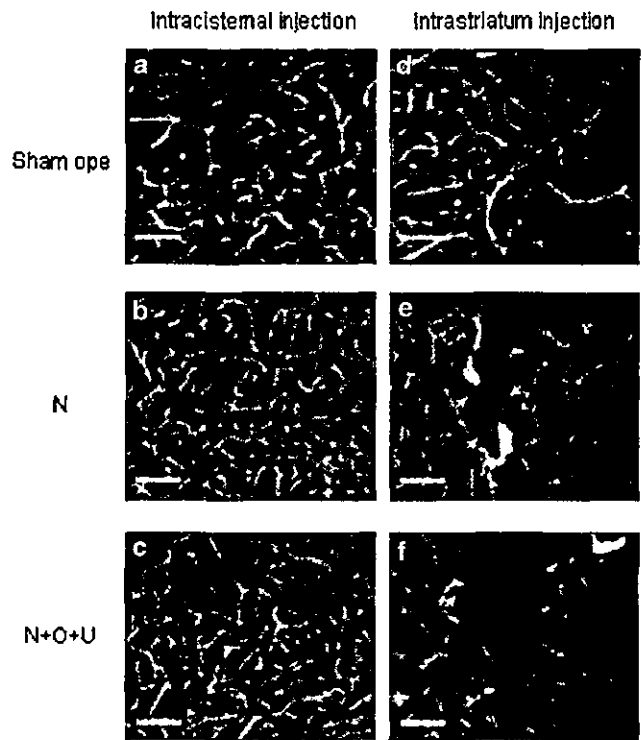
Figure 9 Microangiograms using albumin-fluorescein isothiocyanate at 4 h after injection of naked DNA into cisterna magna or striatum with Optison-enhanced ultrasound method. Confocal microscopic images of vessels in the cerebellum (a–c) and striatum (d–f). There was no leakage of FITC-albumin following intracisternal injection in each group (a–c). Although slight leakage of FITC-albumin was shown after intrastriatal injection, it was not worsened by Optison-enhanced ultrasound. The arrow indicate leakage of FITC-albumin.

into target organs is also important. Recent clinical trials of gene therapy using viral vectors revealed serious problems such as immunogenicity.[5,17] From this viewpoint, application of naked plasmid DNA seems most attractive, as plasmid DNA is very safe as compared to other vectors. However, extremely low transfection efficiency has limited its utility.[10,12] To overcome this problem, we focused on the application of ultrasound, as

enhancement of transfection efficiency using ultrasound has been reported in various tissues such as cardiac muscle,[18] skeletal muscle,[19] carotid artery,[12] and the fetus.[13] Ultrasound-mediated plasmid DNA transfection enhances transfection efficiency, since ultrasound

induces porosity of the cell membrane.[20] Nevertheless, the increased efficiency may still not be enough. Thus, we further modified ultrasound-mediated plasmid DNA transfection using echo-contrast microbubbles. Indeed, the efficiency of plasmid DNA transfection into artery as well as skeletal muscle using ultrasound was reported to be markedly improved by echo-contrast microbubbles, Optison.[12,19] The increase in transfection efficiency might be due to transient holes in the cell membrane produced by the spreading of bubbles.[12]

However, different from other tissues, application of insonation to the adult brain is not easy because of the thick bone of the skull. Although it is well known that pulsed transcranial ultrasound at low frequencies less than 2 MHz can penetrate the human skull and is used to estimate blood flow in the major cerebral vessels, intracerebral ultrasound intensity is thought to be attenuated by the thick skull.[21] Thus, we initially applied this method to the brainstem via the cerebrospinal fluid (CSF) in the cisterna magna, as there is a large window in the bone. As expected, the microbubble-enhanced ultrasound method resulted in marked enhancement of the transfection efficiency as compared to naked plasmid DNA alone. In contrast to previous data using vectors such as adenovirus[22] or HVJ-envelope vector,[23] gene expression was limited to the insonated sites with intracisternal injection. Using the microbubble-enhanced ultrasound method, the transfected cells were mainly meningeal cells, but not neurons or glia. Although we could not clarify the reason why the transfected cells were limited to meningeal cells, one possible reason is that the mixture of naked DNA and Optison might not penetrate into the cerebral parenchyma. Unexpectedly, the span of gene expression by intracisternal injection was shorter than a week. Further studies are needed to achieve longer gene expression.

When naked DNA was injected into the striatum instead of CSF, the transfected cells were mainly glial cells and not neurons, consistent with a previous report.[11] Since glial cells are important for neuronal survival via the secretion of various neurotrophic factors such as fibroblast growth factor (FGF) and hepatocyte growth factor (HGF),[24] gene transfer of neurotrophic factors to glial cells might promote survival of neurons in neurodegenerative diseases such as Parkinson's disease. Alternatively, as a recent report showed that delivery of recombinant GDNF directly into the putamen of five Parkinson's disease patients in a phase I safety trial produced functional improvement,[25] gene transfer might allow long-term production of neuroprotective growth factors, thus resulting in a better outcome.[26] Indeed, gene therapy for Parkinson's disease in animal models also induced functional recovery using an AAV vector[27] or lentiviral vector,[28] although these vectors have several major problems such as immunogenicity. These diseases might be targeted using the microbubble-enhanced ultrasound method, as naked plasmid DNA is much safer and easier to handle.

Although gene transfer using microbubble-enhanced ultrasound was effective, there are some limitations of the present study. First, the effective intensity of ultrasound used in the present study (2 or 5 W/cm^2) was higher than that of commonly used 1 MHz diagnostic ultrasound in the brain (0.5 W/cm^2). While there was no significant adverse effect of Optison and

ultrasound on histological findings and BBB function at the injection site, the possibility of hemorrhage, BBB destruction, or an inflammatory response in other regions could not be completely excluded. Also, the possibility of damage to bone and soft tissue has not been excluded, since they were not evaluated in the present study. Since 185 kHz ultrasound insonation (2 W/cm^2) was reported to potentiate transcranial ultrasound-improved thrombolysis without tissue damage,[29] the ultrasound parameters such as frequency still need to be optimized. Second, we did not examine other echo contrast microbubbles such as Levovist, since they were reported not to enhance the transfer efficiency into cultured human vascular smooth muscle cells and endothelial cells.[12] However, as the biological conditions might differ between *in vivo* and *in vitro* or among tissues, further studies are necessary to investigate which kind of echo contrast microbubbles is best. Third, as we did not examine lower (6.25 or 12.5%) or higher doses (50%) of Optison with other conditions of ultrasound, further studies are necessary to clarify the optimal combination of Optison and ultrasound. Fourth, we dissolved a large amount of plasmid DNA in TE buffer, which is a hypo-osmolar solution and known to be toxic to the CNS. The solvent and amount of plasmid DNA need to be optimized for clinical use in the future.

Overall, the present study demonstrated a safe and efficient method of nonviral gene transfer into the adult central nervous system. As no significant body weight loss, BBB dysfunction, or histological change was observed throughout the experimental period, these data clearly demonstrate the clinical utility of a therapeutic strategy based on plasmid DNA-mediated transfer. What is the clinical relevance of a highly efficient gene transfer method based on plasmid DNA using ultrasound with Optison? First, it is possible to decrease the amount of plasmid DNA, thereby decreasing the potential side effects and cost. Second, it is possible to achieve high transfection efficiency without a viral vector. Avoiding a viral gene transfer method such as by use of an adenovirus may increase the safety of gene therapy and extend its application to a wide variety of targeted diseases. Third, further modification of delivery tools such as a catheter with ultrasound may expand the utility of the present modification to transfection into the adult brain. Although the achieved expression of the transgene was still not particularly high in the present study, more effective expression of transgene might be achieved by optimizing these factors.

Materials and methods

Plasmid DNA

pCMV-luciferase-GL3 (pcLuc-GL3: 7.4 kb) was constructed by cloning the luciferase gene from the pGL3-promoter vector (Promega Corp., Madison, WI, USA) into pcDNA3 (5.4 kb) (Invitrogen, San Diego, CA, USA) at the *Hin*dIII and *Bam*HI sites. Plasmid DNA was purified with a QIAGEN plasmid isolation kit (Hilden, Germany). Venus/pCS2 (4.1 kb) was constructed by insertion of the CMV promoter into the Venus gene at the *Bam*HI and *Eco*RI sites in pCS2. Venus/pCS2 was donated by Dr Miyawaki[30] (Laboratory for Cell Function

and Dynamics, Advanced Technology Development Center, Brain Science Institute, RIKEN, Japan).

Preparation of naked DNA–microbubble mixture

Supercoiled plasmid DNA was dissolved in TE buffer. Optison (Mallinckrodt Inc., San Diego, CA, USA) was used for microbubbles. The plasmid–microbubble solution was prepared just before injection. For intracisternal injection, a total volume of 100 µl containing 200 µg plasmid and Optison (0, 6.25, 12.5, 25, or 50 µl) was used. For intrastriatal injection, a total volume of 6 µl containing 50 µg plasmid and 1.5 µl Optison was used.

In vivo gene transfer in normal rats

Male Wistar rats (230–260 g; Charles River Japan, Atsugi, Japan) were used in this study. All procedures were conducted in accordance with Osaka University guidelines. Rats were anesthetized by intraperitoneal injection of a mixture of ketamine (Sankyo, Tokyo, Japan) and xylazine (Bayer, Tokyo, Japan). For infusion into the subarachnoid space, the head of each animal was fixed in a prone position, and the atlanto-occipital membrane was exposed through an occipitocerebral midline incision. A stainless-steel cannula (27 gauge; Beckton Dickinson) was introduced into the cisterna magna (subarachnoid space). Plasmid DNA solution was infused at 50 µl/min using an injector (IM-3, Narishige Scientific Instrument Laboratory, Tokyo, Japan) after removing 100 µl CSF. Then, animals were exposed to ultrasound from the injection site or temporal bone (Figure 1a–c).

For infusion into the striatum, animals were placed in a stereotactic frame (Narishige Scientific Instrument Laboratory, Tokyo, Japan) with the skull exposed. A stainless-steel cannula (33 gauge) was introduced into the striatum (0.2 mm anterior to the bregma, 3.0 mm lateral to the midline, and 5.0 mm below the skull surface). Plasmid DNA solution was injected at 2.0 µl/min using the injector. Rats were kept in the same position for 3 min to avoid loss of plasmid by backflow. Then, the animals were insonated from the parietal bone (Figure 1d and e).

The ultrasound-emitting transducer used in the present study was an Ultax UX-301 (Celcom Inc., Fukuoka, Japan) with contact gel. The ultrasound parameters were as described previously,[12,13] with minor modifications: the transducer diameter was 29 mm, the central frequency was 1 MHz continuous wave (CW), the duty cycle was 26% (on cycles/off cycles = 26/74, pulse repetition frequency = 2 Hz), the intensity was up to 5 W/cm^2, and acoustic pressure was 0.55 MPa. Animals were exposed once in each experiment immediately after injection of naked DNA.

Assay for luciferase activity

Animals transfected with the luciferase gene were killed under anesthesia at 24 h after transfection. Tissues were harvested and placed individually in FALCON 50 ml tubes. Luciferase activity assay was performed as described previously.[31] Luciferase levels were normalized by determining the protein concentrations of the tissue extracts.[31] Luciferase activity was expressed as relative light units (RLU) per gram of tissue protein. To examine the efficacy of ultrasound-mediated gene transfer via the subarachnoid space, we divided the

brain into brain stem and cerebellum, left hemisphere, right hemisphere, and olfactory bulb. For gene transfer after intrastriatal injection, the right hemisphere (injected hemisphere) was cut at 3.0 mm anterior to the bregma and 3.0 mm posterior to the bregma, after division of the brain into left and right hemispheres.

Determination of fluorescence of Venus and immunohistochemical staining

At 3 days after transfection, animals were killed by perfusion with 150 ml physiological saline, followed by 200 ml 4% paraformaldehyde in physiological saline. The brain was removed and fixed in the same fixative for 16 h. The brain was sectioned at 40 µm on a vibratome. For immunohistochemical staining, free-floating sections were incubated in 0.1% Triton X-100, 3% normal goat serum, and anti-NeuN (1:1000, Chemicon, Temecula, CA, USA) after blocking, followed by anti-rabbit fluorescent antibody (1:1000, Alexa Flour 546-conjugated goat anti-mouse IgG, Molecular Probes, OR, USA). The sections were mounted with VECTA SHIELD (Vector Laboratories, Burlingame, CA, USA). Expression of Venus and immunohistochemical staining were examined under a confocal laser microscope (Bio-Rad, Hercules, CA, USA).

Histological staining

To investigate tissue damage, animals were killed by perfusion with 150 ml physiological saline 4 h or 28 days after each treatment. The brain was removed and fixed in the same fixative for 24 h and embedded in paraffin. Sections were cut at 8 µm at 11.6, 12.6, 13.6, 14.6, and 15.6 mm posterior to the bregma in the case of intracisternal injection or at the injection site in the case of intrastriatal injection, and then subjected to hematoxylin and eosin staining. To evaluate BBB function, we used a recently developed microangiographic technique.[16] This technique allows evaluation of BBB function as well as vascular pattern. Briefly, fluorescent albumin solution was prepared by reconstituting 500 mg bovine desiccate albumin-fluorescein isothiocyanate (Sigma-Aldrich, USA) in 50 ml PBS. The solution was injected via the jugular vein at a rate of 1 ml/min (10 ml/kg) 4 h after treatment. The same amount of blood was withdrawn before the injection to avoid systemic blood pressure elevation. The brain was fixed in 10% formalin solution and then cryoprotected. The brain was cut in the coronal plane at 50 µm using a freezing microtome and mounted with VECTA SHIELD. We set the region of interest (ROI) at the cerebellum and medulla oblongata or striatum. Five consecutive sections in each rat were observed using a confocal laser microscope (Bio-Rad). BBB leakage could be determined by visualization of albumin.[16]

References

1 Eck SL et al. Treatment of recurrent or progressive malignant glioma with a recombinant adenovirus expressing human interferon-beta (H5.010CMVhIFN- beta): a phase 1 trial. Hum Gene Ther 2001; 12: 97–113.

2 Trask TW et al. Phase I study of adenoviral delivery of the HSV-tk gene and ganciclovir administration in patients with current malignant brain tumors. Mol Ther 2000; 1: 195–203.

3 During MJ, Kaplitt MG, Stern MB, Eidelberg D. Subthalamic GAD gene transfer in Parkinson disease patients who are candidates for deep brain stimulation. Hum Gene Ther 2001; 12: 1589–1591.

4 Janson C et al. Clinical protocol. Gene therapy of Canavan disease: AAV-2 vector for neurosurgical delivery of aspartoacylase gene (ASPA) to the human brain. Hum Gene Ther 2002; 13: 1391–1412.

5 Schnell MA et al. Activation of innate immunity in nonhuman primates following intraportal administration of adenoviral vectors. Mol Ther 2001; 3: 708–722.

6 Dewey RA et al. Chronic brain inflammation and persistent herpes simplex virus 1 thymidine kinase expression in survivors of syngeneic glioma treated by adenovirus-mediated gene therapy: implications for clinical trials. Nat Med 1999; 5: 1256–1263.

7 Hsich G, Sena-Esteves M, Breakefield XO. Critical issues in gene therapy for neurologic disease. Hum Gene Ther 2002; 13: 579–604.

8 Baumgartner I et al. Lower-extremity edema associated with gene transfer of naked DNA encoding vascular endothelial growth factor. Ann Intern Med 2000; 132: 880–884.

9 Rosengart TK et al. Angiogenesis gene therapy: phase I assessment of direct intramyocardial administration of an adenovirus vector expressing VEGF121 cDNA to individuals with clinically significant severe coronary artery disease. Circulation 1999; 100: 468–474.

10 Schwartz B et al. Gene transfer by naked DNA into adult mouse brain. Gene Therapy 1996; 3: 405–411.

11 Sekiguchi K, Yasuzumi F, Morishita R. Exogenous expression of hepatocyte growth factor (HGF) in rat striatum by naked plasmid DNA. Neurosci Res 2003; 45: 173–180.

12 Taniyama Y et al. Local delivery of plasmid DNA into rat carotid artery using ultrasound. Circulation 2002; 105: 1233–1239.

13 Endoh M et al. Fetal gene transfer by intrauterine injection with microbubble-enhanced ultrasound. Mol Ther 2002; 5: 501–508.

14 Mychaskiw II G et al. Optison (FS069) disrupts the blood–brain barrier in rats. Anesth Analg 2000; 91: 798–803.

15 Hynynen K et al. The threshold for brain damage in rabbits induced by bursts of ultrasound in the presence of an ultrasound contrast agent (Optison). Ultrasound Med Biol 2003; 29: 473–481.

16 Cavaglia M et al. Regional variation in brain capillary density and vascular response to ischemia. Brain Res 2001; 910: 81–93.

17 Somia N, Verma IM. Gene therapy: trials and tribulations. Nat Rev Genet 2000; 1: 91–99.

18 Unger EC, Hersh E, Vannan M, McCreery T. Gene delivery using ultrasound contrast agents. Echocardiography 2001; 18: 355–361.

19 Taniyama Y et al. Development of safe and efficient novel nonviral gene transfer using ultrasound: enhancement of transfection efficiency of naked plasmid DNA in skeletal muscle. Gene Therapy 2002; 9: 372–380.

20 Tachibana K et al. Induction of cell-membrane porosity by ultrasound. Lancet 1999; 353: 1409.

21 Daffertshofer M, Fatar M. Therapeutic ultrasound in ischemic stroke treatment: experimental evidence. Eur J Ultrasound 2002; 16: 121–130.

22 Yukawa H et al. Adenoviral gene transfer of basic fibroblast growth factor promotes angiogenesis in rat brain. Gene Therapy 2000; 7: 942–949.

23 Shimamura M et al. HVJ-envelope vector for gene transfer into central nervous system. Biochem Biophys Res Commun 2003; 2: 464–471.

24 Albrecht PJ et al. Ciliary neurotrophic factor activates spinal cord astrocytes, stimulating their production and release of fibroblast growth factor-2, to increase motor neuron survival. Exp Neurol 2002; 173: 46–62.

25 Gill SS et al. Direct brain infusion of glial cell line-derived neurotrophic factor in Parkinson disease. Nat Med 2003; 9: 589–595.

26 Kordower JH. In vivo gene delivery of glial cell line-derived neurotrophic factor for Parkinson's disease. Ann Neurol 2003; 53: S120–S132; discussion S132–S134.

27 Wang L et al. Delayed delivery of AAV-GDNF prevents nigral neurodegeneration and promotes functional recovery in a rat model of Parkinson's disease. Gene Therapy 2002; 9: 381–389.

28 Georgievska B et al. Neuroprotection in the rat Parkinson model by intrastriatal GDNF gene transfer using a lentiviral vector. Neuroreport 2002; 13: 75–82.

29 Behrens S et al. Transcranial ultrasound-improved thrombolysis: diagnostic versus therapeutic ultrasound. Ultrasound Med Biol 2001; 27: 1683–1689.

30 Nagai T et al. A variant of yellow fluorescent protein with fast and efficient maturation for cell-biological applications. Nat Biotechnol 2002; 20: 87–90.

31 Tsujie M et al. Electroporation-mediated gene transfer that targets glomeruli. J Am Soc Nephrol 2001; 12: 949–954.

Enhanced Tumor-Specific Long-Term Immunity of Hemaggluttinating Virus of Japan-Mediated Dendritic Cell-Tumor Fused Cell Vaccination by Coadministration with CpG Oligodeoxynucleotides[1]

Kazuya Hiraoka,*[†] Seiji Yamamoto,* Satoru Otsuru,* Seiji Nakai,* Katsuto Tamai,* Ryuichi Morishita,[‡] Toshio Ogihara,[†] and Yasufumi Kaneda[2]*

Immunization with dendritic cells (DCs) using various Ag-loading approaches has shown promising results in tumor-specific immunotherapy and immunoprevention. Fused cells (FCs) that are generated from DCs and tumor cells are one of effective cancer vaccines because both known and unknown tumor Ags are presented on the FCs and recognized by T cells. In this study, we attempted to augment antitumor immunity by the combination of DC-tumor FC vaccination with immunostimulatory oligodeoxynucleotides containing CpG motif (CpG ODN). Murine DCs were fused with syngeneic tumor cells ex vivo using inactivated hemagglutinating virus of Japan (Sendai virus). Mice were intradermally (i.d.) immunized with FCs and/or CpG ODN. Coadministration of CpG ODN enhanced the phenotypical maturation of FCs and unfused DCs, and the production of Th1 cytokines, such as IFN-γ and IL-12, leading to the induction of tumor-specific CTLs without falling into T cell anergy. In addition, immunization with FCs + CpG ODN provided significant protection against lethal s.c. tumor challenge and spontaneous lung metastasis compared with that with either FCs or CpG ODN alone. Furthermore, among mice that rejected tumor challenge, the mice immunized with FCs + CpG ODN, but not the mice immunized with FCs or CpG ODN alone, completely rejected tumor rechallenge, indicating that CpG ODN provided long-term maintenance of tumor-specific immunity induced by FCs. Thus, the combination of DC-tumor FCs and CpG ODN is an effective and feasible cancer vaccine to prevent the generation and recurrence of cancers. *The Journal of Immunology,* 2004, 173: 4297–4307.

A lthough surgery, chemotherapy, and radiotherapy are effective cancer treatments, some cancers are refractory to these treatments. Effective treatment of advanced and metastatic cancers and the prevention of recurrence are especially difficult. Immunotherapy and immunoprevention are promising approaches to cancer treatment and prevention that may someday overcome the shortcomings of traditional cancer managements.

Two different signals are required to prime and activate naive CD4^{+} and CD8^{+} T cells (1). First, antigenic peptides must be presented on the surface of activated APCs by MHC class I or II molecules to CD8^{+} or CD4^{+} T cells, respectively. The binding of peptide/MHC complexes to TCRs mediates a signal into the T cells. A second signal must be mediated from costimulatory molecules on activated APCs to T cells. Thus, it is essential for cancer vaccines to activate APCs, such as dendritic cells (DCs),[3] that can recognize and present tumor Ags to T cells (2).

Tumor-associated Ags (TAAs) presented by mature DCs are needed to evoke tumor-specific immune response. Several melanoma Ags recognized by T cells have been identified, including MAGE, gp100, MART-1, TRP-1, TRP-2, and tyrosinase (3). DCs treated with TAA peptides or tumor lysates enhanced tumor immunity in melanoma patients (4). TAAs have also been identified in cancers other than melanoma (5). However, TAAs in many cancers have not been identified.

To solve this problem, hybrid cell vaccines have been developed by fusing mature DCs with tumor cells. DC-tumor fused cells (FCs) express known and unknown TAAs, as well as high levels of MHC class I and II molecules and costimulatory molecules that can prime and activate naive CD4^{+} and CD8^{+} T cells (6). Therefore, even though tumor cells lose the expression of MHC class I molecules, TAAs can be presented on the surface of FCs by DC-derived MHC class I molecules.

It has been reported that vaccinations of mice with DC-tumor FCs induce therapeutic and protective immune responses against established and spontaneous tumors, which included both immunogenic and poorly immunogenic tumors (7–12). In these studies, FCs were generated by polyethylene glycol (PEG) (7–10) or electrofusion (11, 12). In vitro studies using human cells have shown that DC-tumor FCs present both known and unknown TAAs in the context of HLA class I molecules and induce tumor-specific CTL response (10). In clinical trials, patients with malignant glioma (13) or melanoma (14) were vaccinated with autologous DC-tumor

FCs generated by PEG. These vaccinations were safe, but only induced weak clinical responses.

TAA alone is not sufficient for producing effective vaccines, and the aid of adjuvants to enhance vaccine effects has been pointed out (15). Adjuvants play an important role in determining the quality and quantity of immune response to Ags. Many adjuvants including recombinant Th1 cytokines, such as IL-2 and IL-12, as well as Freund's adjuvant, aluminum salts, and monophosphoryl lipid have been used in animals and humans (16). However, these adjuvants resulted in little or no immune enhancement and caused toxicity in some cases.

Recently, synthetic oligodeoxynucleotides containing specific bacterial unmethylated CpG motif (CpG ODN), which are one of so-called pathogen-associated molecular patterns, have attracted a great deal of attention as a novel and safe adjuvant (17–19). CpG ODN are recognized by cells of innate immune system of vertebrates, such as B cells, macrophages, monocytes, and DCs, and activate these cells (17, 18). CpG ODN preferentially induce Th1 immune response through its receptor, TLR9, with the production of cytokines, such as TNF-α, IL-12, and IFN-γ, appropriate for the development of antitumor immunity (20). Indeed, the use of CpG ODN as an adjuvant combined with other immunotherapies, such as TAA peptide-pulsed DCs (21), or as a monotherapy (22) induced antitumor response in mice, while TAA peptide-pulsed DCs alone were not effective. The effect of CpG ODN on human cancers is currently being evaluated in clinical trials (23).

Several studies of DC-tumor FC vaccines in mice have reported that coadministration of FCs with rIL-2 (8) or IL-12 (9, 11) by i.p. injection as an adjuvant enhances the antitumor effect more effectively compared with that induced by either FCs or the adjuvant alone. These results suggest the need of adjuvant to enhance antitumor immunity in the use of FCs for cancer vaccines.

In this study, we investigated whether CpG ODN could safely enhance tumor-specific immune response induced by DC-tumor FC vaccines generated by inactivated hemagglutinating virus of Japan (HVJ; Sendai virus).

Materials and Methods

Materials

All cell lines, including B16BL6 melanoma (H-2^b), EL4 T cell lymphoma (H-2^b), RENCA renal cell carcinoma (H-2^d), and CT26 colon adenocarcinoma (H-2^d), were purchased from American Type Culture Collection (Manassas, VA). Synthesized ODN, such as phosphorothioate-modified CpG ODN (CpG 1668; 5'-TCCAT GACGTTCCTGATGCT-3') and non-CpG ODN (GpG 1668; 5'-TCCATGAGGTTCCTGATGCT-3') (18), were purchased from Hokkaido System Science (Sapporo, Japan). Male 8-wk-old C57BL/6 (H-2^b) and BALB/c (H-2^d) mice were purchased from Oriental Yeast (Tokyo, Japan) and maintained in a temperature-controlled, pathogen-free room. All animals were handled according to approved protocols and the guidelines of the Animal Committee of Osaka University.

Preparation and culture of DCs

Murine bone marrow-derived DCs were generated as previously described (24) with minor modifications (25). Briefly, after flushing out bone marrow of tibia and femur with RPMI 1640 medium, effluent tissue was passed through 40-μm mesh, and erythrocytes were lysed with ammonium chloride. After washing, 1×10^6 cells were plated in 24-well plates (Costar, Corning, NY) in 1 ml of RPMI 1640 medium supplemented with 10% heat-inactivated FBS (Equitech-Bio, Kerrville, TX), antibiotics, 50 μM 2-ME, and 10 ng/ml recombinant murine GM-CSF (Genzyme-Techne, Minneap-

olis, MN). The cultures were fed every other day by gentle pipetting, aspirating all of the medium, and adding fresh medium. On day 6 of culture, nonadherent and loosely adherent clusters of proliferating DCs were collected, and 1×10^6 cells were replated in 24-well plates in 1 ml of DC medium with 100 ng/ml LPS (*Escherichia coli* 055:B5) (Sigma-Aldrich, St. Louis, MO) for 24 h. On day 7 of culture, nonadherent DCs were harvested and used for fusion. More than 90% of these DCs were positive for CD11c and displayed a typical mature phenotype as confirmed by flow cytometry.

HVJ-mediated cell fusion

HVJ (Z strain) was purified from chorioallantoic fluid of chick eggs by centrifugation, and the titer was calculated as previously described (26). The virus was inactivated by UV irradiation (99 mJ/cm^2) just before use. With this preparation, the ability of virus replication was lost completely, but fusion activity was not affected as previously described (27). To determine optimal fusion efficiency, mature DCs and tumor cells were labeled with fluorescent red and green, respectively, using PKH26 and PKH67 according to the manufacturer's instructions (Zynaxis Cell Science, Malvern, PA). PKH dyes were intensively washed to remove the unbound dyes and to avoid leakage of the bound dyes between DCs and tumor cells. Alternatively, mature DCs and B16BL6 cells were labeled with FITC-conjugated anti-mouse mAb against CD11c and anti-human gp100 primary mAb (DakoCytomation, Glostrup, Denmark) followed by PE-conjugated anti-mouse κ L chain secondary mAb (BD Pharmingen, San Diego, CA), respectively. FITC mAbs against CD40, CD80, CD86, or MHC class II were also used as DC markers. The tumor cells were then irradiated with 100 Gy using ^{137}Cs gamma rays generated by Gammacell (MDS Nordion, Ottawa, Ontario, Canada) and fused with mature DCs at a ratio of 1:2 using HVJ as previously described (28) with some modifications. Briefly, mature DCs (4×10^6 cells) suspended in 250 μl of balanced salt solution (BSS; 10 mM Tris-Cl (pH 7.5), 137 mM NaCl, 5.4 mM KCl) containing 2 mM CaCl$_2$ and irradiated tumor cells (2×10^6 cells) suspended in 250 μl of BSS containing 2 mM CaCl$_2$ and various amounts of HVJ (0–1000 hemagglutinating units (HAU)) suspended in 500 μl of BSS were mixed in a 2-ml tube. After incubation at 0°C for 5 min, the mixture was incubated at 37°C for 15 min with shaking (120 rpm) in a water bath to induce cell-cell fusion. After centrifugation at 1200 rpm for 3 min at 4°C, the fusion products were washed twice with 1.5 ml of BSS to remove the free HVJ and cultured overnight at 37°C in 5% CO$_2$. After 24-h culture following fusion, the fusion products were harvested. Fusion efficiency was evaluated with FACScan and FACSVantage (BD Biosciences, San Jose, CA). FCs collected using FACSVantage (BD Biosciences) were subjected to some experiments.

Phenotypic analysis

After fusion between nonlabeled mature DCs and PKH26-labeled B16BL6 cells using 500 HAU of inactivated HVJ, the fusion products were cultured for 24 h with or without 10 μg/ml CpG ODN, followed by staining with FITC mAbs against CD11c, CD40, CD80, CD86, or MHC class II as DC markers. Surface phenotypes of FCs were analyzed by gating and excluding single red-positive cells using FACSVantage (BD Biosciences).

Immunization in vivo

After 12-h incubation of fusion products generated from DCs and irradiated syngeneic tumor cells (B16BL6 or RENCA cells) using 0 HAU (i.e., Mix) or 500 HAU (i.e., FCs) of HVJ, 6×10^6 cells were harvested and suspended in 200 μl of PBS. CpG ODN (100

μg) was dissolved in 100 μl of PBS and mixed with 100 μl of PBS (i.e., CpG alone) or 6 $\times$ 10^6 cells suspended in 100 μl of PBS (i.e., Mix + CpG and FCs + CpG) immediately before injection into mice. In some experiments, FCs were collected with a cell sorter, and 1.2 $\times$ 10^6 FCs (i.e., sorted FCs) were injected into mice. The mice (10 mice/group) were immunized twice, at weekly intervals as reported previously (9, 29, 30), with one of these vaccination protocols in a total volume of 200 μl of PBS by i.d. injection into the bilateral posterior flanks near the base of the tail (100 μl per flank). We selected this route of immunization because FCs migrate into draining lymph nodes after i.d. injection (31, 32). The number of cells in the fusion products was described based on the number of cells that were used in the DC-tumor cell fusion.

Cytokine measurements

After 24-h incubation of fusion products generated by 0 HAU (i.e., Mix) or 500 HAU (i.e., FCs) of HVJ with or without 10 μg/ml CpG ODN, the supernatants were harvested before immunization and stored at $-80°$C. After in vivo immunization, cell culture supernatants of isolated spleen cells on day 5 during restimulation were also collected and stored at $-80°$C. The concentrations of TNF-α, IL-12 p40, IFN-γ, and IL-4 in the supernatants were measured by ELISA Development kits (Genzyme-Techne).

Cytolytic assay

Ten days after the second immunization, spleen cells were pooled from each group of mice (three mice per group). The spleen cells (5 $\times$ 10^6 cells/well) were cocultured to restimulate with mitomycin C-treated tumor cells at a ratio of 20:1 in 2 ml of T cell culture medium (RPMI 1640 medium supplemented with 10% heat-inactivated FBS, antibiotics, and 50 μM 2-ME) in 24-well plates at 37°C in 5% CO_2. The cells, which contained CTLs, were harvested on day 5 and used as effector cells in a standard 4-h ^{51}Cr release assay to examine antitumor cytolytic activity. Briefly, target tumor cells (1 $\times$ 10^6) were labeled with 100 μCi of $Na_2^{51}CrO_4$ (Amersham Biosciences, Buckinghamshire, U.K.) in 200 μl of RPMI 1640 supplemented with 10% heat-inactivated FBS for 90 min at 37°C. The labeled target cells (1 $\times$ 10^4 cells/well) were incubated with the effector cells for 4 h at 37°C in 96-well microtiter plates in 200 μl of T cell medium at various E:T ratios. The plates were then centrifuged, and the radioactivity of the supernatants was counted using a MicroBeta Trilux Scintillation Counter (Wallac, Gaithersburg, MD). The maximum or spontaneous release was defined as counts from samples incubated with 2% Triton X-100 or medium alone, respectively. Cytolytic activity was calculated using the following formula: percentage of specific ^{51}Cr release = (experimental release $-$ spontaneous release) $\times$ 100/(maximum release $-$ spontaneous release). Assays were performed in triplicate wells. The spontaneous release in all assays was <20% of the maximum release.

Prophylactic treatment in s.c. tumor model

Ten days after the second vaccination, C57BL/6 mice were challenged by s.c. injection with 1 $\times$ 10^5 B16BL6 cells, and BALB/c mice were injected s.c. with 1 $\times$ 10^5 RENCA cells into the back different, but proximal, from two vaccinated sites. After tumor challenge, mice were monitored daily. Tumor incidence was considered positive when the tumor length exceeded 3 mm. Tumor size was measured every other day in a blinded manner with digital calipers. Tumor volume was calculated using the following formula: tumor volume (mm^3) = length $\times$ (width)^2/2 (Ref. 33). Mice were euthanized when tumors became ulcerated or surpassed 4000 mm^3 in volume. Sixty days after tumor inoculation, tumor-free C57BL/6 or BALB/c mice were rechallenged s.c. with 1 $\times$ 10^5

B16BL6 cells and 5 $\times$ 10^4 EL4 cells or 1 $\times$ 10^5 RENCA cells and 5 $\times$ 10^4 CT26 cells, respectively, injected into the back to clarify tumor specificity of the vaccination in vivo.

Prophylactic treatment in spontaneous lung metastasis model

B16BL6 melanoma cells are highly invasive and spontaneously metastatic from the primary site (34). Ten days after the second vaccination, C57BL/6 mice (eight mice per group) were injected s.c. with 5 $\times$ 10^5 B16BL6 cells suspended in 50 μl of PBS into the right hind footpad to initiate primary tumor growth. On day 21 after tumor inoculation, when the primary tumor was >10 mm in length, it was surgically removed by a right hip disarticulation with removal of the regional draining popliteal and inguinal lymph nodes. All mice were euthanized 21 days after surgery, and the lungs were fixed in Bouin's solution (Sigma-Aldrich). The number of lung metastases was counted under a dissecting microscope (35).

Statistical analysis

Statistical analysis was performed with StatView software (Abacus Concepts, Berkeley, CA). The χ^2 test was used to analyze differences between percentages of tumor-free mice at day 60. The log-rank test was used to analyze Kaplan-Meier survival curves. The unpaired Fisher's protected least significant difference test was used in other analyses. We defined statistical significance as $p < 0.05$.

Results

HVJ-mediated DC-tumor cell fusion

We used inactivated HVJ to generate DC-tumor FCs. Murine DCs (4 $\times$ 10^6 cells) stained with PKH26 (shown in red) and irradiated B16BL6 cells (2 $\times$ 10^6 cells) stained with PKH67 (shown in green) were fused with UV-inactivated HVJ. After 24-h incubation, the fusion products were analyzed by flow cytometry. Fluorescent microscopic observation after sorting each fraction revealed that double-positive cells in the upper right fraction were large and fluorescent yellow DC-tumor FCs, while the lower right and upper left fractions contained unfused B16BL6 cells and DCs, respectively (Fig. 1A).

To determine the optimal fusion conditions, fusion efficiency and cell viability of fusion products generated by various amounts of HVJ (0–1000 HAU) were investigated. Fusion efficiency analyzed by flow cytometry was 5.38, 13.71, 25.49, and 26.57% with 0, 100, 500, and 1000 HAU of inactivated HVJ, respectively (Fig. 1B). Spontaneous double-positive cells were obtained at low efficiency (5.38%) even in the absence of HVJ, maybe resulting from the capture of irradiated tumor cells by DCs (Fig. 1B, 0 HAU). Cell viability assessed by lactose dehydrogenase release assay was 96, 93, 85, and 60% after 24-h culture following fusion, and 74, 67, 60, and 25% after 72-h culture following fusion with 0, 100, 500, and 1000 HAU, respectively (500 HAU vs 1000 HAU, $p < 0.05$). We obtained similar results for fusion efficiency and cell viability in at least 10 separate experiments. Therefore, we chose 500 HAU of inactivated HVJ to generate DC-tumor FCs in the following experiments.

Furthermore, we analyzed the expression of specific markers derived from DCs and B16BL6 melanoma cells in DC-tumor FCs. FACS analysis (Fig. 2A) showed that, with 500 HAU of inactivated HVJ, cells expressing both DC surface markers such as CD11c, CD40, CD80, CD86, or MHC class II and B16BL6 marker, gp100, were generated at ~30% efficiency. Without HVJ (indicated as 0 HAU in Fig. 2A), cells with both surface markers were 3–9% in this assay. Fluorescent microscopic observation of the fusion products generated from DCs stained with FITC mAb against CD11c (Fig. 2B, left panel), a DC marker, and B16BL6

FIGURE 1. HVJ-mediated DC-tumor cell fusion. *A*, Fusion protocol. Bone marrow-derived DCs (4 × 10⁶ cells) stained with PKH26 (red) and irradiated B16BL6 cells (2 × 10⁶ cells) stained with PKH67 (shown in green) were mixed at a 2:1 ratio, and fused with UV-inactivated HVJ. The free HVJ was removed by centrifugation and washing with BSS, and the cells were cultured at 37°C in 5% CO_2. After 24-h incubation, the fusion products were collected. Double-positive (*upper right*), single green-positive (*lower right*), and single red-positive cells (*upper left*) were sorted using flow cytometry and observed by fluorescent microscopy (magnification, ×100). *B*, Fusion efficiency. Various amounts of HVJ (0–1000 HAU) were used to fuse DCs stained with PH26 (shown in red) and irradiated B16BL6 cells stained with PKH67 (shown in green). The fusion efficiency was assessed by flow cytometry. Fluorescence microscopy was used to demonstrate DC-B16BL6 FCs, shown as large yellow cells (magnification, ×200).
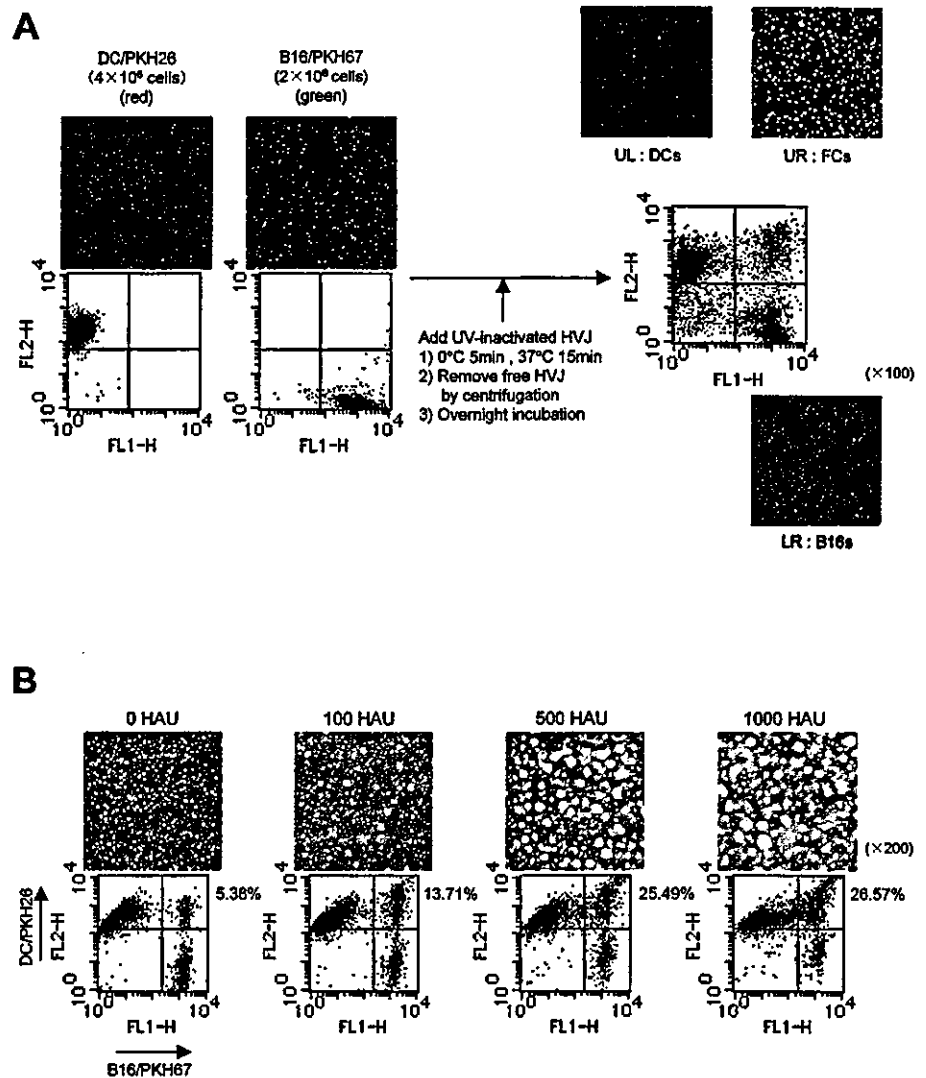
cells stained with PE mAb against gp100 TAA (Fig. *2B, center panel*), a B16BL6 cell marker, showed that DC-B16BL6 FCs were positive for both markers (Fig. *2B, right panel*). These findings indicate that inactivated HVJ could be used as a fusogen for DC-tumor cell fusion.

*Enhanced phenotypical maturation and Th1 cytokine production of FCs by administration with CpG ODN in vitro*

We analyzed the phenotypical maturation of FCs containing unfused DCs by examining the expression of various surface markers of DCs. The expression of surface markers of DCs was up-regulated by the treatment with 100 ng/ml LPS, and maintained in FCs after fusion (Fig. 3A). The phenotypical maturation of FCs was further enhanced by 10 μg/ml CpG ODN, especially in CD80, CD86, and MHC class II (Fig. 3A). We also analyzed the production of Th1 cytokines, such as TNF-α and IL-12, from the mixture of mature DCs and B16BL6 cells (Mix) or FCs. FCs produced significantly more TNF-α than Mix (Fig. 3B). The production of IL-12 p40 was comparable between FCs and Mix (Fig. 3C). The amount of both cytokines produced by FCs or Mix was approximately doubled when CpG ODN were administered with the cells. However, non-CpG ODN did not enhance the production of these cytokines (Fig. 3, B and C). The highest production of these cytokines was obtained in the supernatants of FCs incubated with 10 μg/ml CpG ODN (FCs + CpG). CpG ODN did not affect the

viability of FCs (data not shown). We also found that mature DCs treated with inactivated HVJ did not enhance the cytokine production (data not shown). These results indicate that CpG ODN, but not inactivated HVJ, could promote further phenotypical maturation and activation of FCs.

Enhanced tumor-specific immune response of FCs by coadministration with CpG ODN in vivo

To assess whether tumor-specific CTLs were induced after immunization with FCs, two parameters of effector function, IFN-γ and IL-4 production and cytolytic activity, were investigated (Fig. 4). IFN-γ secreted from spleen cells on day 5 during restimulation with B16BL6 cells was highest when the mice were vaccinated with the combination of FCs and CpG ODN (FCs + CpG; Fig. 4A). To examine cytokine production from only FCs, we sorted DC-tumor hybrid cells using a cell sorter. IFN-γ production in sorted FCs was similar to that in FCs in the absence of CpG ODN. Furthermore, the production of IFN-γ in sorted FCs was enhanced with CpG ODN as much as that in FCs. Although the production of Th2 cytokine, IL-4, was also enhanced with either FCs or sorted FCs, the amount was much less than IFN-γ.

Cytolytic activity of spleen cells from the mice immunized with FCs was significantly higher compared with that from other vaccination protocols, such as PBS, CpG, Mix, and Mix + CpG (Fig. 4B). Furthermore, the highest cytolytic activity was observed in
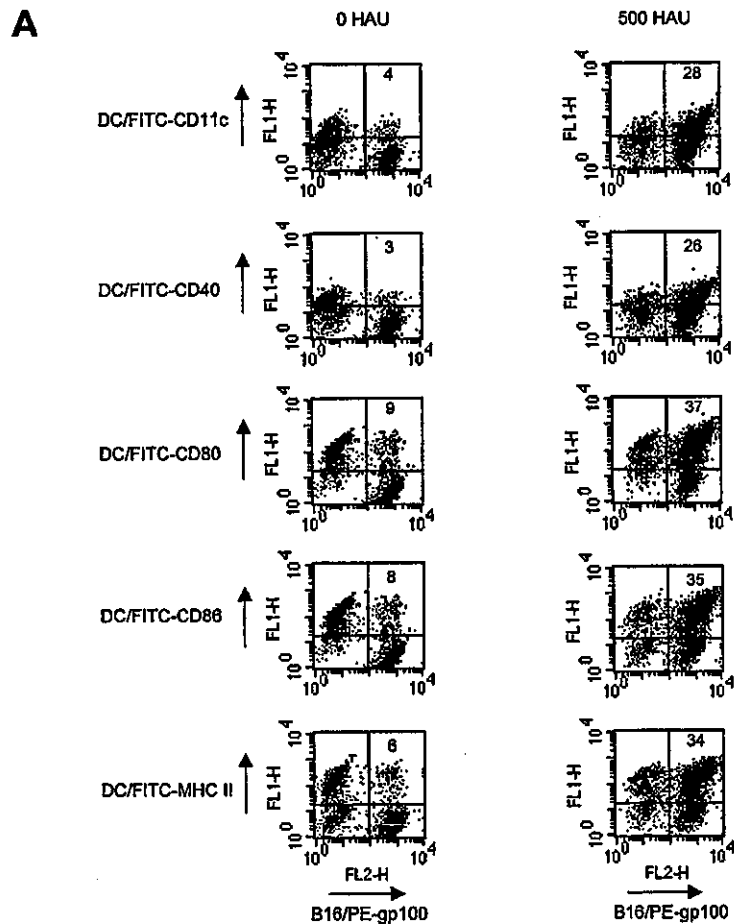
FIGURE 2. Characterization of DC-tumor FCs. *A,* FACS analysis of DC-tumor FCs generated by inactivated HVJ. After 24-h incubation of fusion products with (500 HAU) or without (0 HAU) inactivated HVJ, surface phenotypes of DCs and gp100 expression of B16BL6 were analyzed by flow cytometry. Each number indicates the percentage of double-positive cells. These experiments were repeated twice with similar results. *B,* Identification of DC-tumor FCs with specific markers. After 24-h culture of fusion products generated from DCs, stained with FITC mAb against CD11c (*left*) as a DC marker, and B16BL6 cells, stained with PE mAb against gp100 TAA (*center*) as a B16BL6 cell marker, fluorescent microscopy showed that DC-B16BL6 FCs were double-positive cells expressing both markers (*right*) with ~20% fusion efficiency. White arrows indicate DC-B16BL6 FCs (magnification, ×400).
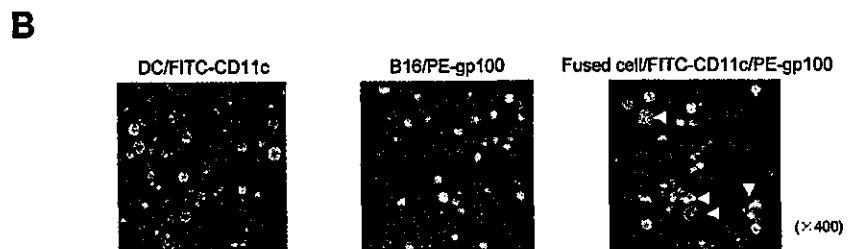
the mice that received FCs + CpG compared with that in the mice that received FCs alone (Fig. 4B). No cytolytic effect was observed when other syngeneic tumor cells, EL4 T cell lymphoma cells, were used as the target cells (Fig. 4C). These results indicate that CpG ODN strongly enhanced the tumor-specific immune response generated by FCs.

Enhanced prophylactic effect of FCs coadministered with CpG ODN on the growth of mouse tumors

The effect of vaccination with FCs + CpG on the inhibition of s.c. tumor growth was investigated in a melanoma model (Fig. 5). After the challenge with 1 × 10⁵ B16BL6 cells, mice immunized with FCs + CpG significantly inhibited tumor growth compared with mice that received either FCs or CpG ODN alone (Fig. 5A). When mice were immunized with sorted FCs, tumor growth was similarly inhibited as immunized with FCs, and the inhibition of tumor growth was also enhanced with CpG ODN (Fig. 5A). Mice vaccinated with FCs + CpG significantly increased survival times. Eighty percent of mice vaccinated with FCs + CpG were alive 60 days after tumor challenge, while only 20% of mice immunized with FCs alone were still alive and all mice in the other groups

died (Fig. 5B). Furthermore, 6 of 10 mice vaccinated with FCs + CpG remained tumor free 60 days after tumor injection, whereas none of the mice immunized with FCs alone was tumor free in the B16BL6 tumor model (Fig. 5C).

We also examined the effect of vaccination with FCs + CpG on the enhancement of tumor-specific immunity against murine RENCA tumors in which TAAs have not been identified (Fig. 6). Mice vaccinated with FCs generated from DCs and RENCA cells had greater IFN-γ secretion than mice immunized with the mixture without fusion (Mix). IFN-γ secretion was enhanced by coadministration with CpG ODN (Fig. 6A). Tumor-specific CTLs were also generated and the highest cytolytic activity was obtained by vaccination with FCs + CpG (Fig. 6, *B* and *C*). Sixty days after tumor challenge with RENCA cells, 8 of 10 mice vaccinated with FCs + CpG were tumor free, while 5 of 10 mice immunized with FCs alone were tumor free and no mice from the other vaccination groups were tumor free (Fig. 6D). Similar results were obtained in two other experiments (Table I, Tumor-free mice/mice 1st challenged).

Therefore, immunization with FCs + CpG strongly induced Th1 cytokines and activated tumor-specific CTLs, resulting in the
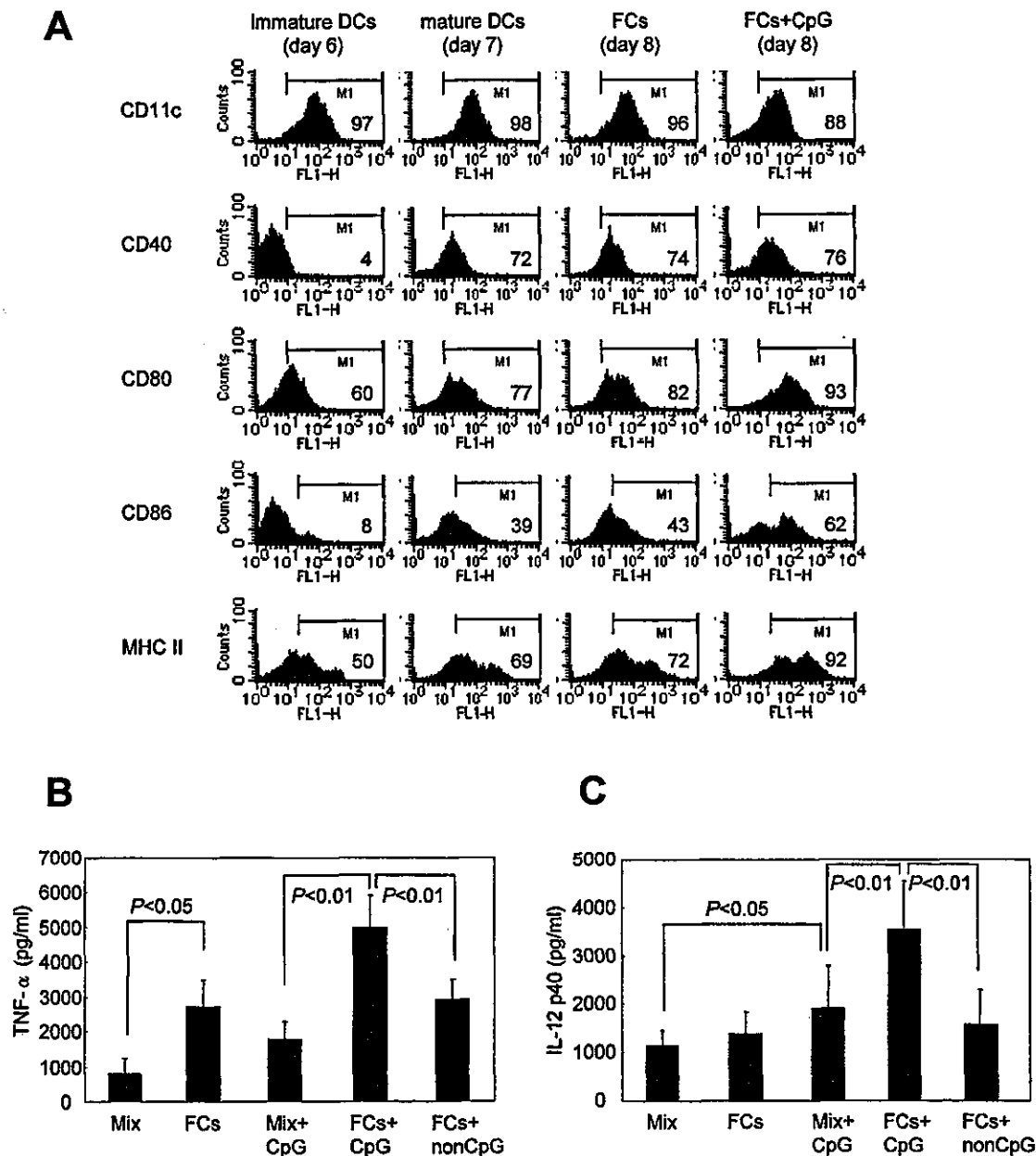
FIGURE 3. Enhanced phenotypical maturation and Th1 cytokine production of FCs in combination with CpG ODN in vitro. *A*, Surface phenotype. After 24-h incubation of fusion products with (FCs + CpG) or without (FCs) 10 μg/ml CpG ODN, surface phenotypes of DC-tumor FCs were gated and analyzed by flow cytometry. Phenotypes of immature and LPS-prestimulated mature DCs are shown as controls. Each number indicates the percentage of positive cells. These experiments were repeated twice with similar results. *B* and *C*, Th1 cytokine production. TNF-α (*B*) and IL-12 p40 (*C*) in the supernatants of either mixture (Mix) of DCs and tumor cells or DC-tumor FCs were measured with ELISA kits. The effect of 10 μg/ml CpG ODN on cytokine production was assessed. Non-CpG ODN were used as a control. Data are presented as the mean ± SD of four independent experiments.

significantly sufficient protection against B16BL6 tumors, in which TAAs have been identified, and RENCA tumors, in which TAAs are unknown.

*Inhibition of lung metastasis by FCs in combination with CpG ODN*

The effect of vaccination with FCs + CpG on the inhibition of lung metastasis was further investigated. B16BL6 cells were injected into the right hind footpad of vaccinated mice. On day 21 after tumor inoculation, the primary tumor was surgically removed. All mice were euthanized 21 days after surgery, and the number of lung metastases of melanoma was counted in the eight mice. The number of metastatic foci was significantly reduced by vaccination

with FCs (Fig. 7). Moreover, mice immunized with FCs + CpG further inhibited lung metastases as compared with either FCs alone or Mix + CpG (Fig. 7).

Enhanced long-lasting immune response of FCs by coadministration with CpG ODN

Our results indicated that CpG ODN strongly enhanced tumor-specific immune response of FCs. We finally investigated whether CpG ODN maintain tumor-specific immunity of FCs. Six of 10 mice in the B16BL6 tumor model and 8 of 10 mice in the RENCA tumor model that received vaccination with FCs + CpG remained tumor free for 60 days after the first tumor injection (Figs. 5C and 6D). These mice were rechallenged with the same tumor cells used

FIGURE 4. Enhanced B16BL6 cell-specific immune response of FCs coinjected with CpG ODN in vivo. A, IFN-γ and IL-4 production. Mice vaccinated with either FCs '+ CpG or sorted FCs + CpG had significantly higher IFN-γ concentration in the supernatants from spleen cell cultures on day 5 during restimulation. Data are presented as the mean ± SD of three independent experiments. B and C, Cytolytic assay. Ten days after the second immunization, spleen cells isolated from vaccinated mice were cocultured with mitomycin C-treated B16BL6 cells for 5 days and used as effector cells in 4-h ^{51}Cr release assay. Significantly higher cytolytic activity was observed in the mice that received FCs + CpG (B), whereas no cytolytic effect was observed when EL4 cells were used as the target cells (C). Data are presented as the mean ± SD of triplicate samples of one representative experiment. These experiments were repeated twice with similar results.
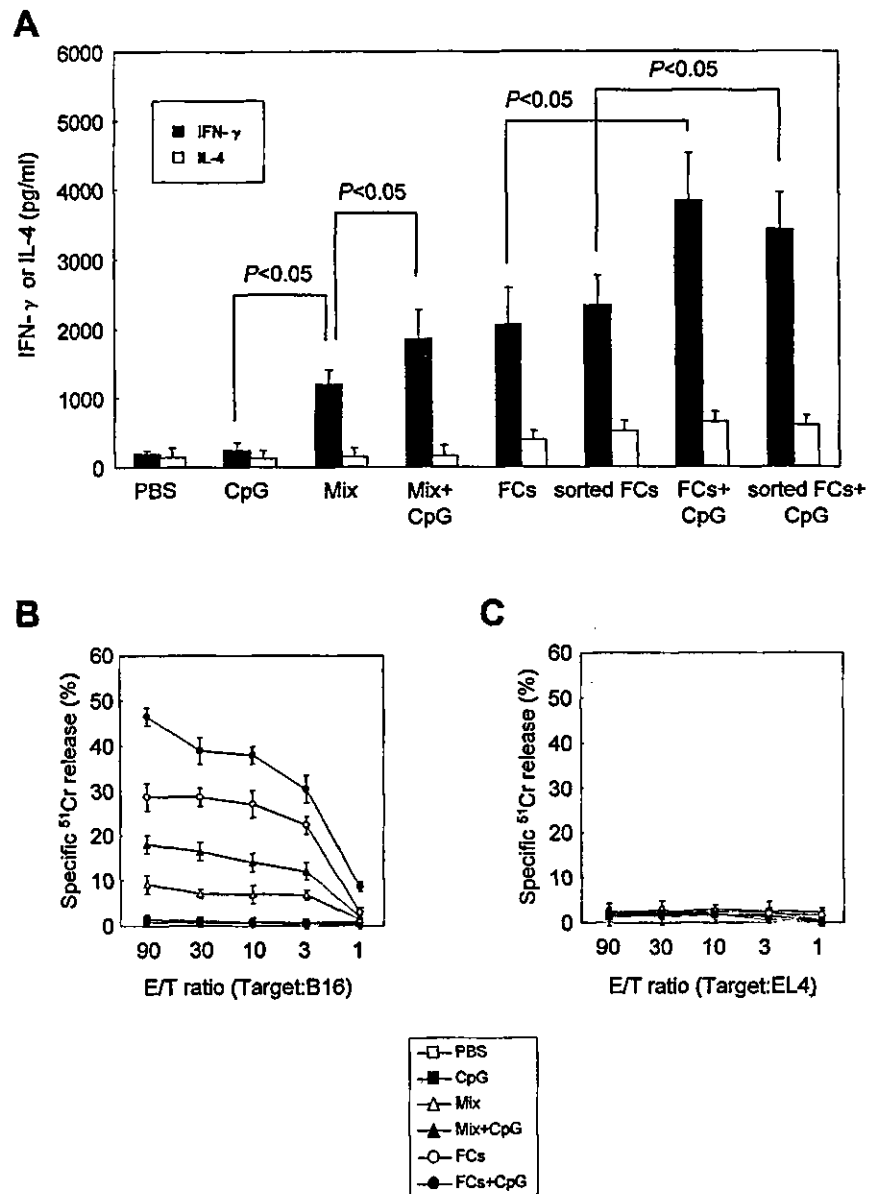
for the first challenge or with other syngeneic tumor cells. All mice immunized with FCs + CpG completely rejected tumor rechallenge with the same tumor cells (B16BL6 or RENCA cells) and remained tumor free for 60 days after the second tumor injection (Table I), while the mice did not reject other syngeneic tumor cells (EL4 or CT26 cells). However, among five BALB/c mice that rejected the first tumor challenge with RENCA cells by immunization with FCs alone (Fig. 6D), only two mice rejected tumor rechallenge with the same tumor cells and three mice developed RENCA tumors (Table I, Expt. 1). Similar results were obtained in two other experiments (Table I). These findings indicate that CpG ODN could enhance long-lasting tumor-specific immunity generated by FCs. FCs in the absence of CpG ODN did not maintain tumor-specific immunity so effectively as FCs + CpG ODN, resulting in incomplete protection against tumor rechallenge.

Discussion

In this study, we demonstrated that a new vaccination strategy of HVJ-mediated DC-tumor FCs in combination with CpG ODN induced tumor-specific and long-term immunity against two different murine tumors.

A number of studies have reported that DC-tumor FCs induce tumor-specific immune response (7–12). These studies suggested that the effective presentation of both known and unknown TAAs is feasible with DC-tumor FCs. Our study also supports the utility of DC-tumor cell fusion for eliciting antitumor immunity. In this study, we used inactivated HVJ as a fusogen. Under optimal fusion conditions, HVJ generated 20–30% of DC-tumor FCs with low toxicity, accompanied by few or no DC-DC or tumor-tumor FCs (Fig. 1, A and B). The fusion efficiency using HVJ was comparable to the previously reported fusion efficiency of PEG (7–10) and electrofusion (11, 12). However, in our hands, fusion efficiency between DC and tumor cells and the viability of FCs using PEG was very low (<10 and 40%, respectively). The PEG fusion method is technically challenging. It has been reported that it is difficult to determine optimal conditions for effective electrofusion with low toxicity (11, 12). Thus, HVJ-mediated cell fusion appeared to be simpler and more reproducible than other fusion methods.

Two distinct glycoproteins of HVJ are required for cell fusion (26). Hemagglutinin neuraminidase protein binds to sialic acid receptors on the cell surface and degrades the receptor by sialidase
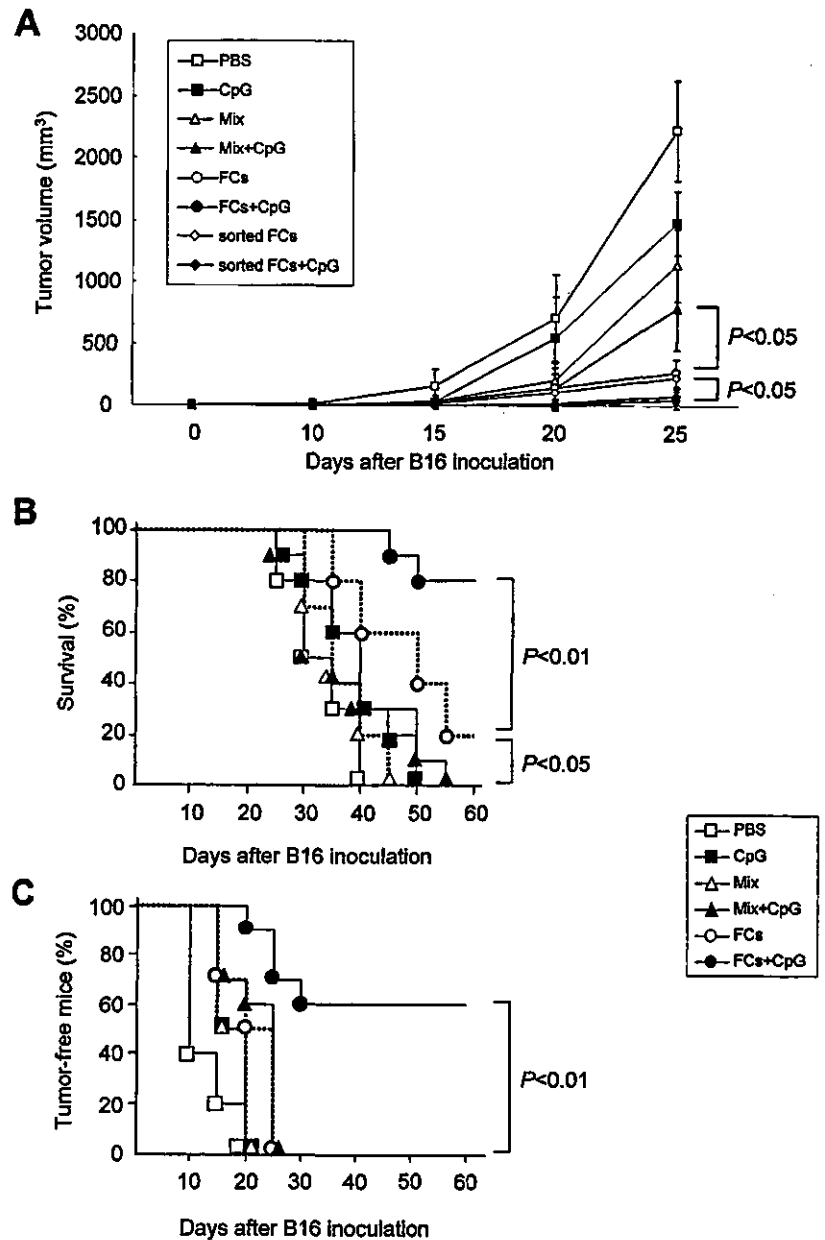
FIGURE 5. Inhibition of melanoma growth in mice using FCs combined with CpG ODN. The antitumor effect of the vaccinations with CpG ODN in combination with the mixture of DCs and tumor cells (Mix) or DC-tumor FCs was examined in the prophylactic model. C57BL/6 mice (10 mice per group) were pre-immunized twice i.d. with PBS (□), CpG ODN (■), Mix (△), Mix + CpG (▲), FCs (○), FCs + CpG (●), sorted FCs (◇), or sorted FCs + CpG (◆). Ten days after the second immunization, these mice were challenged by s.c. injection of 1×10^5 B16BL6 cells into the back on day 0. A, The growth of B16BL6 after s.c. inoculation into vaccinated mice. Data are presented as the mean tumor volume ± SD. B, The percentage of surviving mice after tumor injection. C, The ratio of tumor-free mice after tumor injection. These experiments were repeated twice with similar results.

activity. Fusion protein then associates with lipid molecules, such as cholesterol, on the cell surface to induce cell fusion. Recently, Phan et al. (32) developed a new method to generate DC-tumor FCs based on gene transfer of a fusogenic glycoprotein derived from vesicular stomatitis virus into tumor cells. This report supports our DC-tumor cell fusion method using viral fusion proteins, such as hemagglutinin neuraminidase and fusion proteins, of HVJ.

DC-tumor FCs possess properties that include both known and unknown TAAs derived from tumor cells, as well as necessary levels of MHC, costimulatory molecules, and probably other components derived from DCs (Fig. 2, A and B). The rationale for using DC-tumor FCs as a cancer vaccine is to raise T cells directed against the whole antigenic repertoire of the tumor cells (6). Because tumors escape from immunosurveillance through the down-regulation of MHC class I or TAA expression (36), it is likely that successful vaccination for immunotherapy or immunoprevention against tumors requires multiple tumor Ags like a polyvalent vaccine (37). DC-tumor FCs appear to be ideal cancer vaccines because various kinds of TAAs can be presented by MHC class I

molecules derived from DCs, even though tumor cells lose the expression of MHC class I molecules and some TAAs (6, 38).

Because it is necessary to trigger innate immunity for subsequent effective acquired immunity (20), we attempted to enhance the antitumor activity induced by immunization with DC-tumor FCs by using CpG ODN as an adjuvant. CpG ODN are recognized by TLR9 mainly in DCs, leading to activation of the innate immune system, which includes DCs, macrophages, and NK cells (20). Because DC-tumor FCs possessed properties of both DCs and tumor cells (Fig. 2B), we expected that TLR9 expressed in DCs could also be expressed in DC-tumor FCs, and therefore, CpG ODN could directly stimulate these cells. Indeed, we found that CpG ODN enhanced the phenotypical maturation and Th1 cytokine production of FCs, but not of the mixture without fusion, indicating that FCs themselves might be activated by CpG ODN through TLR9.

We observed that repeated i.d. administration of CpG ODN alone was safe, but failed to protect mice against subsequent tumor challenge as previously reported (39), indicating that, especially in

FIGURE 6. Enhanced RENCA cell-specific immune response of FCs by coadministration with CpG ODN in vivo. BALB/c mice (10 mice per group) were preimmunized twice i.d. with PBS (□), CpG ODN (■), Mix (△), Mix + CpG (▲), FCs (○), or FCs + CpG (●). Ten days after the second immunization, these mice were challenged by s.c. injection of 1×10^5 RENCA cells into the back on day 0. A, IFN-γ and IL-4 production. The mice that received FCs + CpG vaccination had significantly higher IFN-γ concentration in the supernatants from spleen cell cultures on day 5 during restimulation. Data are presented as the mean ± SD of three independent experiments. B and C, Cytolytic assay. Cytolytic activity was assessed by specific ^{51}Cr release from RENCA cells (B) and CT26 cells (C). Data are presented as the mean ± SD of triplicate samples of one representative experiment. D, The ratio of tumor-free mice after the injection of RENCA cells. These experiments were repeated three times with similar results.
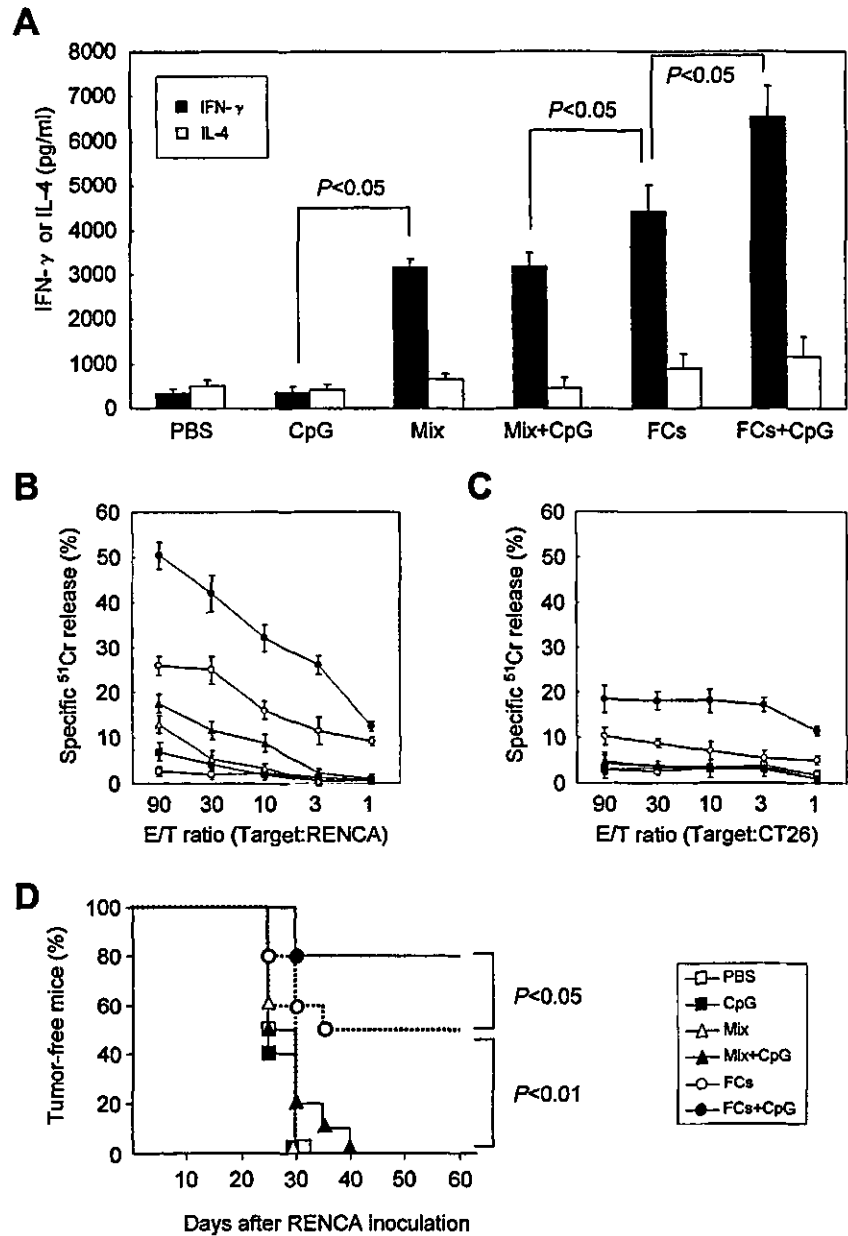
prophylactic use, CpG ODN alone induce only nonspecific expansion of the innate immune cells (40). In contrast, we demonstrated that i.d. immunization with FCs, but not the mixture of DCs and tumor cells, induced higher tumor-specific cytolytic activity and provided significant protection against tumor challenge. We found that vaccination with fusion products generated from either DCs alone, which contain DC-DC FCs, or tumor cells alone, which contain tumor-tumor FCs, did not protect mice (data not shown).

Table I. Complete induction of tumor-specific long-term immunity after tumor rechallenge in mice immunized with FCs plus CpG ODN[a]

Mice	Tumor Cell 1st Challenged	Preimmunization Tumor-Free Mice/ Mice 1st Challenged[b]	Tumor Cell 2nd Challenged	Tumor-Free Mice/Mice 2nd Challenged[c]
C57/BL6	B16	FCs 0/10 (0%), 0/10 (0%), 0/10 (0%)		
		FCs + CpG 6/10 (60%), 4/10 (40%), 5/10 (50%)	B16 EL4	3/3 (100%), 2/2 (100%), 3/3 (100%) 0/3 (0%), 0/2 (0%), 0/2 (0%)
BALB/c	RENCA	FCs 5/10 (50%), 6/10 (60%), 4/10 (40%)	RENCA	2/5 (40%), 3/6 (50%), 1/4 (25%)
		FCs + CpG 8/10 (80%), 9/10 (90%), 6/10 (60%)	RENCA CT26	4/4 (100%), 5/5 (100%), 3/3 (100%) 0/4 (0%), 0/4 (0%), 0/3 (0%)

[a] This table represents the results of three independent experiments (Expt. 1, Expt. 2, Expt. 3).
[b] The ratio of tumor-free mice on day 60 after the first tumor challenge.
[c] The ratio of tumor-free mice on day 60 after the second tumor challenge.
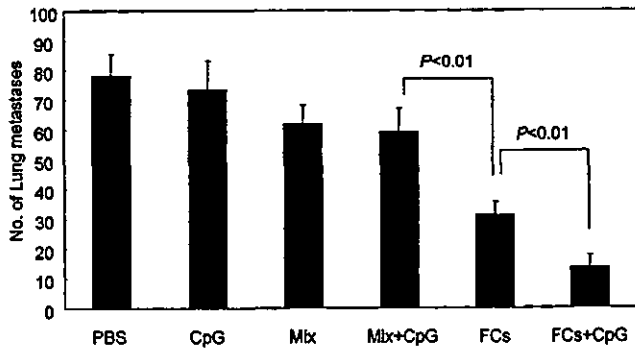
FIGURE 7. Inhibition of lung metastasis by FCs in combination with CpG ODN. The effect of various vaccinations on the inhibition of lung metastasis was investigated. Ten days after the second vaccination, C57BL/6 mice (eight mice per group) were s.c. injected with 5×10^5 B16BL6 cells into the right hind footpad. On day 21 after tumor inoculation, the primary tumor was surgically removed. All mice were euthanized 21 days after surgery, and the number of lung metastatic foci in each mouse is shown. Data are presented as the mean ± SD of three independent experiments.

Additionally, in the combination with or without CpG ODN, antitumor activity of 6×10^6 FCs containing both fused and unfused cells was comparable to that of 1.2×10^6 sorted FCs (Figs. 4A and 5A). These findings indicate that DC-tumor FC fraction, which only exists in the FCs, is required to elicit the antitumor effect. Moreover, we revealed that i.d. immunization with CpG ODN in combination with FCs, but not with the mixture, further enhanced tumor-specific immune response generated by FCs. CpG ODN might enhance cross-presentation of TAAs by both FCs (38) and unfused DCs (41), leading to effective activation of MHC class I-restricted CTLs. The results of cytolytic assay indicate that CD8$^+$ CTLs are mainly involved in the tumor-specific cytolytic activity, at least through IFN-γ release induced by the vaccination with FCs in combination with or without CpG ODN. However, cytolytic activity against CT26 cells was observed in spleen cells from the mice vaccinated with FCs between DCs and RENCA tumor cells in combination with CpG ODN (Fig. 6C), although the activity was much lower than that against RENCA cells. This result suggests that NK cells might also participate in this response to some extent. This speculation is supported by previous reports showing that both CD8$^+$ and NK cells (29, 30), in addition to CD4$^+$ cells (7), are activated by the immunization with FCs between DCs and tumor cells, and that both CD8$^+$ and NK cells mediate CpG ODN-induced antitumor immune response (42).

We demonstrated that CpG ODN provided long-term maintenance of tumor-specific immunity induced by FCs, leading to complete rejection of tumor rechallenge (Table I). Although the precise mechanisms by which CpG ODN are capable of maintaining the antitumor effect generated by FCs are unknown, several possibilities can be explored. Effective antitumor immunity generally requires CD4$^+$ Th cells, which participate in further activation of DCs through CD40-CD40L interaction and subsequent induction of CD8$^+$ effector CTL response (1). However, it is also indicated that effector CTLs can be induced without CD4$^+$ Th cells (43). The induction of CD4$^+$ Th cell-independent CTL function may also occur in DC-tumor FC vaccines. However, in terms of maintenance after the induction of effector CTLs, recent studies have reported that CD4$^+$ T cell help plays a critical role in the development and activation of functional CD8$^+$ memory T cells (44, 45). It has also been recently reported that CpG ODN not only enhance but also maintain CD8$^+$ effector CTL response through

the expansion, inhibition of apoptosis, and subsequent promotion of long-term survival of CD8$^+$ effector and memory T cells (40, 46). Especially, the expansion and survival of memory CD8$^+$ T cells have been reported to be mediated by IL-15 (47), which is produced by DCs in response to type I IFN (48). CpG ODN stimulate DCs to produce type I IFN (49). Taken together, we estimated that in our experiments, CD4$^+$, CD8$^+$, and NK cells would play a key role in the activation and enhancement of long-lasting tumor-specific immune response by the immunization with FCs + CpG ODN.

Moreover, the generation of humoral response against tumors using hybrid cell vaccine has been already reported in several papers (9, 50), and the significance of antimelanoma Ab after the injection of TAA genes has been also reported (51). Therefore, it is estimated that the humoral response against tumors might be also induced by the vaccination with FCs or FCs + CpG ODN.

From the viewpoint of cancer immunoprevention, this combination vaccine is ideal because the presentation of many MHC-restricted known and unknown TAAs or Ags presented by the MHC-independent pathway on FCs as well as the long-lasting effect of CpG ODN on tumor-specific immunity are very useful to avoid the selection of TAA-loss variants and to recognize MHC-loss variants in the generation and recurrence of cancer (52).

In the surviving mice immunized twice with FCs in combination with CpG ODN and challenged with B16BL6 cells, no apparent inflammation, such as autoimmune skin depigmentation (vitiligo), was observed. Only localized hair loss in the area surrounding the tumor injection site was observed. Similar findings were observed in the surviving mice from the RENCA tumor model. These findings suggest that repeated vaccinations with FCs in combination with CpG ODN are safe and feasible for clinical immunotherapy and immunoprevention against cancers. This safety is essential for clinical use as a cancer immunoprevention vaccine.

In conclusion, we have developed a simple and reproducible method to generate DC-tumor FCs using inactivated HVJ. Vaccination of HVJ-mediated DC-tumor FCs in combination with CpG ODN induced tumor-specific and long-term immunity in the prophylactic setting of a s.c. tumor model and a spontaneous lung metastasis model, resulting in significant inhibition of tumor incidence and prolongation of survival time. CpG ODN could strongly enhance and maintain tumor-specific immune response induced by DC-tumor FC vaccines in vivo. We hope that this type of immunoprevention can eventually be tested in human clinical trials to inhibit cancer recurrence and micrometastasis after surgery.

References

1. Banchereau, J., and R. M. Steinman. 1998. Dendritic cells and the control of immunity. *Nature* 392:245.
2. Pardoll, D. M. 1998. Cancer vaccines. *Nat. Med. 4:525.*
3. Boon, T., J. C. Cerottini, B. Van den Eynde, P. van der Bruggen, and A. Van Pel. 1994. Tumor antigens recognized by T lymphocytes. *Annu. Rev. Immunol. 12:337.*
4. Nestle, F. O., S. Alijagic, M. Gilliet, Y. Sun, S. Grabbe, R. Dummer, G. Burg, and D. Schadendorf. 1998. Vaccination of melanoma patients with peptide- or tumor lysate-pulsed dendritic cells. *Nat. Med. 4:328.*
5. Kawakami, Y., and S. A. Rosenberg. 1997. Human tumor antigens recognized by T-cells. *Immunol. Res. 16:313.*
6. Kufe, D. W. 2000. Smallpox, polio and now a cancer vaccine? *Nat. Med. 6:252.*
7. Gong, J., D. Chen, M. Kashiwaba, and D. Kufe. 1997. Induction of antitumor activity by immunization with fusions of dendritic and carcinoma cells. *Nat. Med. 3:558.*
8. Wang, J., S. Saffold, X. Cao, J. Krauss, and W. Chen. 1998. Eliciting T cell immunity against poorly immunogenic tumors by immunization with dendritic cell-tumor fusion vaccines. *J. Immunol. 161:5516.*
9. Gong, J., S. Koido, D. Chen, Y. Tanaka, L. Huang, D. Avigan, K. Anderson, T. Ohno, and D. Kufe. 2002. Immunization against murine multiple myeloma with fusions of dendritic and plasmacytoma cells is potentiated by interleukin 12. *Blood 99:2512.*

10. Chan, R. C., H. Xie, G. P. Zhao, and Y. Xie. 2002. Dendritomas formed by fusion of mature dendritic cells with allogenic human hepatocellular carcinoma cells activate autologous cytotoxic T lymphocytes. *Immunol. Lett. 83:101.*

11. Hayashi, T., H. Tanaka, J. Tanaka, R. Wang, B. J. Averbook, P. A. Cohen, and S. Shu. 2002. Immunogenicity and therapeutic efficacy of dendritic-tumor hybrid cells generated by electrofusion. *Clin. Immunol. 104:14.*

12. Siders, W. M., K. L. Vergilis, C. Johnson, J. Shields, and J. M. Kaplan. 2003. Induction of specific antitumor immunity in the mouse with the electrofusion product of tumor cells and dendritic cells. *Mol. Ther. 7:498.*

13. Kikuchi, T., Y. Akasaki, M. Irie, S. Homma, T. Abe, and T. Ohno. 2001. Results of a phase I clinical trial of vaccination of glioma patients with fusions of dendritic and glioma cells. *Cancer Immunol. Immunother. 50:337.*

14. Krause, S. W., C. Neumann, A. Soruri, S. Mayer, J. H. Peters, and R. Andreesen. 2002. The treatment of patients with disseminated malignant melanoma by vaccination with autologous cell hybrids of tumor cells and dendritic cells. *J. Immunother. 25:421.*

15. Lutz, M. B., and G. Schuler. 2002. Immature, semi-mature and fully mature dendritic cells: which signals induce tolerance or immunity? *Trends Immunol. 23:445.*

16. Parmiani, G., C. Castelli, P. Dalerba, R. Mortarini, L. Rivoltini, F. M. Marincola, and A. Anichini. 2002. Cancer immunotherapy with peptide-based vaccines: what have we achieved? Where are we going? *J. Natl. Cancer Inst. 94:805.*

17. Krieg, A. M. 2003. CpG motifs: the active ingredient in bacterial extracts? *Nat. Med. 9:831.*

18. Krieg, A. M., A. K. Yi, S. Matson, T. J. Waldschmidt, G. A. Bishop, R. Teasdale, G. A. Koretzky, and D. M. Klinman. 1995. CpG motifs in bacterial DNA trigger direct B-cell activation. *Nature 374:546.*

19. Weeratna, R. D., M. J. McCluskie, Y. Xu, and H. L. Davis. 2000. CpG DNA induces stronger immune responses with less toxicity than other adjuvants. *Vaccine 18:1755.*

20. Akira, S., K. Takeda, and T. Kaisho. 2001. Toll-like receptors: critical proteins linking innate and acquired immunity. *Nat. Immunol. 2:675.*

21. Heckelsmiller, K., S. Beck, K. Rall, B. Sipos, A. Schlamp, E. Tuma, S. Rothenfusser, S. Endres, and G. Hartmann. 2002. Combined dendritic cell- and CpG oligonucleotide-based immune therapy cures large murine tumors that resist chemotherapy. *Eur. J. Immunol. 32:3235.*

22. Baines, J., and E. Celis. 2003. Immune-mediated tumor regression induced by CpG-containing oligodeoxynucleotides. *Clin. Cancer Res. 9:2693.*

23. Jiang, W., and D. S. Pisetsky. 2003. Enhancing immunogenicity by CpG DNA. *Curr. Opin. Mol. Ther. 5:180.*

24. Inaba, K., M. Inaba, N. Romani, H. Aya, M. Deguchi, S. Ikehara, S. Muramatsu, and R. M. Steinman. 1992. Generation of large numbers of dendritic cells from mouse bone marrow cultures supplemented with granulocyte/macrophage colony-stimulating factor. *J. Exp. Med. 176:1693.*

25. Kaisho, T., O. Takeuchi, T. Kawai, K. Hoshino, and S. Akira. 2001. Endotoxin-induced maturation of MyD88-deficient dendritic cells. *J. Immunol. 166:5688.*

26. Okada, Y. 1993. Sendai virus-induced cell fusion. *Methods Enzymol. 221:18.*

27. Kaneda, Y., T. Nakajima, T. Nishikawa, S. Yamamoto, H. Ikegami, N. Suzuki, H. Nakamura, R. Morishita, and H. Kotani. 2002. Hemagglutinating virus of Japan (HVJ) envelope vector as a versatile gene delivery system. *Mol. Ther. 6:219.*

28. Miyake, Y., J. Kim, and Y. Okada. 1978. Effects of cytochalasin D on fusion of cells by HVJ (Sendai virus). *Exp. Cell Res. 116:167.*

29. Orentas, R. J., D. Schauer, Q. Bin, and B. D. Johnson. 2001. Electrofusion of a weakly immunogenic neuroblastoma with dendritic cells produces a tumor vaccine. *Cell. Immunol. 213:4.*

30. Akasaki, Y., T. Kikuchi, S. Homma, T. Abe, D. Kofe, and T. Ohno. 2001. Antitumor effect of immunizations with fusions of dendritic and glioma cells in a mouse brain tumor model. *J. Immunother. 24:106.*

31. Koido, S., Y. Tanaka, D. Chen, D. Kufe, and J. Gong. 2002. The kinetics of in vivo priming of CD4 and CD8 T cells by dendritic/tumor fusion cells in MUC1-transgenic mice. *J. Immunol. 168:2111.*

32. Phan, V., F. Errington, S. C. Cheong, T. Kottke, M. Gough, S. Altmann, A. Brandenburger, S. Emery, S. Strome, A. Bateman, et al. 2003. A new genetic method to generate and isolate small, short-lived but highly potent dendritic cell-tumor cell hybrid vaccines. *Nat. Med. 9:1215.*

33. Dethlefsen, L. A., J. M. Prewitt, and M. L. Mendelsohn. 1968. Analysis of tumor growth curves. *J. Natl. Cancer Inst. 40:389.*

34. Poste, G., J. Doll, I. R. Hart, and I. J. Fidler. 1980. In vitro selection of murine B16 melanoma variants with enhanced tissue-invasive properties. *Cancer Res. 40:1636.*

35. Saiki, I., J. Iida, J. Murata, R. Ogawa, N. Nishi, K. Sugimura, S. Tokura, and I. Azuma. 1989. Inhibition of the metastasis of murine malignant melanoma by synthetic polymeric peptides containing core sequences of cell-adhesive molecules. *Cancer Res. 49:3815.*

36. Garcia-Lora, A., I. Algarra, and F. Garrido. 2003. MHC class I antigens, immune surveillance, and tumor immune escape. *J. Cell. Physiol. 195:346.*

37. Morton, D. L., L. J. Foshag, D. S. Hoon, J. A. Nizze, E. Famatiga, L. A. Wanek, C. Chang, D. G. Davtyan, R. K. Gupta, R. Elashoff, et al. 1992. Prolongation of survival in metastatic melanoma after active specific immunotherapy with a new polyvalent melanoma vaccine. *Ann. Surg. 216:463.*

38. Parkhurst, M. R., C. DePan, J. P. Riley, S. A. Rosenberg, and S. Shu. 2003. Hybrids of dendritic cells and tumor cells generated by electrofusion simultaneously present immunodominant epitopes from multiple human tumor-associated antigens in the context of MHC class I and class II molecules. *J. Immunol. 170:5317.*

39. Heckelsmiller, K., K. Rall, S. Beck, A. Schlamp, J. Seiderer, B. Jahrsdorfer, A. Krug, S. Rothenfusser, S. Endres, and G. Hartmann. 2002. Peritumoral CpG DNA elicits a coordinated response of CD8 T cells and innate effectors to cure established tumors in a murine colon carcinoma model. *J. Immunol. 169:3892.*

40. Davila, E., M. G. Velez, C. J. Heppelmann, and E. Celis. 2002. Creating space: an antigen-independent, CpG-induced peripheral expansion of naive and memory T lymphocytes in a full T-cell compartment. *Blood 100:2537.*

41. Warren, T. L., S. K. Bhatia, A. M. Acosta, C. E. Dahle, T. L. Ratliff, A. M. Krieg, and G. J. Weiner. 2000. APC stimulated by CpG oligodeoxynucleotide enhance activation of MHC class I-restricted T cells. *J. Immunol. 165:6244.*

42. Kawarada, Y., R. Ganss, N. Garbi, T. Sacher, B. Arnold, and G. J. Hammerling. 2001. NK$^-$ and CD8$^+$ T cell-mediated eradication of established tumors by peritumoral injection of CpG-containing oligodeoxynucleotides. *J. Immunol. 167:5247.*

43. Shiku, H. 2003. Importance of CD4$^+$ helper T-cells in antitumor immunity. *Int. J. Hematol. 77:435.*

44. Janssen, E. M., E. E. Lemmens, T. Wolfe, U. Christen, M. G. von Herrath, and S. P. Schoenberger. 2003. CD4$^+$ T cells are required for secondary expansion and memory in CD8$^+$ T lymphocytes. *Nature 421:852.*

45. Gao, F. G., V. Khammanivong, W. J. Liu, G. R. Leggatt, I. H. Frazer, and G. J. Fernando. 2002. Antigen-specific CD4$^+$ T-cell help is required to activate a memory CD8$^+$ T cell to a fully functional tumor killer cell. *Cancer Res. 62:6438.*

46. Beloeil, L., M. Tomkowiak, G. Angelov, T. Walzer, P. Dubois, and J. Marvel. 2003. In vivo impact of CpG1826 oligodeoxynucleotide on CD8 T cell primary responses and survival. *J. Immunol. 171:2995.*

47. Lu, J., R. L. Giuntoli, Jr., R. Omiya, H. Kobayashi, R. Kennedy, and E. Celis. 2002. Interleukin 15 promotes antigen-independent in vitro expansion and long-term survival of antitumor cytotoxic T lymphocytes. *Clin. Cancer Res. 8:3877.*

48. Mattei, F., G. Schiavoni, F. Belardelli, and D. F. Tough. 2001. IL-15 is expressed by dendritic cells in response to type I IFN, double-stranded RNA, or lipopolysaccharide and promotes dendritic cell activation. *J. Immunol. 167:1179.*

49. Cho, H. J., T. Hayashi, S. K. Datta, K. Takabayashi, J. H. Van Uden, A. Horner, M. Corr, and E. Raz. 2002. IFN-αβ promote priming of antigen-specific CD8$^+$ and CD4$^+$ T lymphocytes by immunostimulatory DNA-based vaccines. *J. Immunol. 168:4907.*

50. Xia, J., Y. Tanaka, S. Koido, C. Liu, P. Mukherjee, S. J. Gendler, and J. Gong. 2003. Prevention of spontaneous breast carcinoma by prophylactic vaccination with dendritic/tumor fusion cells. *J. Immunol. 170:1980.*

51. Tanaka, M., Y. Kaneda, S. Fujii, T. Yamano, K. Hashimoto, S. K. Huang, and D. S. Hoon. 2002. Induction of a systemic immune response by a polyvalent melanoma-associated antigen DNA vaccine for prevention and treatment of malignant melanoma. *Mol. Ther. 5:291.*

52. Lollini, P. L., and G. Forni. 2003. Cancer immunoprevention: tracking down persistent tumor antigens. *Trends Immunol. 24:62.*

RESEARCH ARTICLE

In vivo transfection of a cis element 'decoy' against signal transducers and activators of the transcription 6 (STAT6) binding site ameliorates the response of contact hypersensitivity

K Sumi[1], H Yokozeki[1], M-H Wu[1], T Satoh[1], Y Kaneda[2], K Takeda[3], S Akira[3] and K Nishioka[1]

[1]Department of Environmental Immunodermatology, Postgraduate School, Tokyo Medical & Dental University, Tokyo, Japan; [2]Department of Gene Therapy, School of Medicine, Osaka University, Osaka, Japan; and [3]Department of Host Defense, Research Institute for Microbial Diseases, Osaka University, Osaka, Japan

We herein demonstrate that STAT6 plays an important role in the induction of not only acute contact hypersensitivity (CHS), but also chronic CHS in a mouse model using STAT6-deficient (STAT6⁻/⁻) mice. We, therefore, determine whether synthetic double-stranded DNA with a high affinity for STAT6 can be introduced in vivo as a decoy cis element to bind the transcriptional factor and block the induction of not only acute CHS but also chronic CHS. Treatment by the transfection of STAT6 decoy oligodeoxynucleotides (ODN), after the induction of 2,4,6-trinitrochlorobenzene or other haptens had a significant inhibitory effect on the induction of both acute CHS and chronic CHS. We thus examined the mechanism of the in vivo effect of the transfection of STAT6 decoy ODN in both acute and chronic CHS. In the histological analysis, the infiltration of eosinophils and degranulated mast cells, and the production of IL-4, IL-6 and eotaxin, but not IFN-γ in the extracts from challenged skin significantly decreased by the transfection of STAT6 decoy ODN. We herein report the first successful in vivo transfer of STAT6 decoy ODN to inhibit acute and chronic CHS, thus providing a new therapeutic strategy not only for the treatment of CHS but also for atopic dermatitis.
Gene Therapy (2004) 0, 000–000. doi:10.1038/sj.gt.3302345

Keywords: contact hypersensitivity; atopic dermatitis; STAT6 decoy; Th2 cytokine

Introduction

Contact hypersensitivity (CHS) responses are mediated by T cells following the epicutaneous application of chemically reactive compounds (haptens) to the skin. CHS is thought to be associated with the activation of T cells of Th (T helper) 1 type. However, the role of Th2 cells in CHS is still not clear. Interleukin-4 (IL-4)/IL-10 secreting CD4+ T cells (Th2) have been demonstrated to negatively regulate the CHS response.[1] Steinbrink et al[2] suggested that CD8+ T cells producing IL-4, -5 and -10 play a downregulatory role. A negative regulatory effect of IL-4 on the CHS responses to trinitrochloronbenzene (TNCB) has been also reported by Guatam et al[3] and Asada et al.[4] These authors observed that IL-4 inhibited the efferent phase of CHS but not the afferent phase.[3,4] In contrast to these reports, IL-4 has been demonstrated to be an essential cytokine during the elicitation phase of CHS by several groups.[5–7] In line with these reports, the CHS response has been reported to be diminished in IL-4-deficient mice at the late phase of the elicitation reaction.[8]

We have recently established STAT6-deficient (STAT6⁻/⁻) mice[9] and demonstrated that STAT6 plays an essential role in the induction of CHS.[10] We also recently reported that not only Th2 cytokines, but also mast cells and IgE are important in the induction of CHS.[11,12] Furthermore, Kitagaki et al[13,14] demonstrated that the repeated elicitation of CHS (chronic CHS) induces a shift in the cutaneous cytokines milieu from a Th1 to a Th2 profile. They demonstrated that an important function of Th2 cells and mast cells in chronic CHS may be to minimize the tissue-damaging effects of Th1 cells by producing Th2 cytokines.[13,14] They concluded that this chronic CHS mouse model could thus play a beneficial role in investigating the pathogenesis of such chronic allergic diseases as atopic dermatitis.[13,14] We, therefore, focused our attention on the role of STAT6 in the pathogenesis of both acute and chronic CHS using STAT6⁻/⁻ mice.

Recently, a decoy strategy has been developed and considered a useful tool as a new class of antigene strategy.[15,16] The transfection of double-stranded oligodeoxynucleotides (ODN) as a decoy corresponding to the cis sequence results in the attenuation of the authenic cis–trans interaction, leading to the removal of trans-factors from the endogeneous cis-element, with a subsequent modulation of gene expression.[15,16] Therefore, this decoy approach enables us to treat diseases by modulating